Marine and Coastal Fisheries: Dynamics, Management, and Ecosystem Science 14:e10206, 2022

ISSN: 1942-5120 online
DOI: 10.1002/mcf2.10206

ARTICLE

Examining Epibenthic Assemblages Associated with Artificial Reefs Using a Species Archetype Approach

Haolin Yu and Guangjie Fang
College of Fisheries, Ocean University of China, Qingdao 266003, China

Kenneth A. Rose
Horn Point Laboratory, University of Maryland Center for Environmental Science, Cambridge, Maryland 21613, USA

Yanli Tang* and Xiefa Song
College of Fisheries, Ocean University of China, Qingdao 266003, China

Abstract

The placement of artificial reefs (ARs) influences, to various degrees, a wide range of epibenthic species, whereas most assessments focus on target or focal species. Methods of capturing the responses of many species can inform management about the full range of likely responses of species to the location and arrangement of ARs. Performing many single-species analyses presents difficulties in interpretation. We used monitoring data from 14 surveys from June 2017 to August 2020 in an area with ARs deployed in the Bohai Sea, China. Both trap and visual census data were collected, and a suite of environmental variables was also collected or estimated for sampled sites and for spatial cells throughout the study area. The data were used to fit a species archetype model (SAM) that relies on the shared responses of species to environmental variables. The many species were grouped into six distinct archetypes. Species membership in the archetypes was confirmed by comparing results to the isometric feature mapping and partitioning around medoids (ISOPAM) approach, which relied on species co-occurrence applied to the same data. The SAM results were also validated by comparing archetypes determined with fitting to predictions from a single survey that was not used in fitting. The six archetypes identified by the SAM had member species that differed in dependence on substrate types, distance to the nearest AR, distance to the nearest gravel, temperature, dissolved oxygen, time since AR deployment, and sampling method. The importance of the environmental variables was assessed by computing the changes in predicted occurrence probabilities of the archetypes when environmental variables were varied with the other environmental variables set at their minimum, mean, maximum, or optimal values. Species archetype modeling provides a valuable approach for predicting occurrence probabilities of epibenthic species assemblages in response to the locations and arrangement of ARs, and results can inform management related to fishing enhancement and conservation.

Artificial reefs (ARs) are common tools for restoring local fisheries (Miller 2002), preventing habitat degradation (Abelson 2006; Miller and Hobbs 2007), and promoting local stock enhancement (van Treeck and Schuhmacher 1999). A wide range of species is affected by the placement of ARs, including pelagic (Becker et al.

*Corresponding author: tangyanli@ouc.edu.cn
Received October 28, 2021; accepted March 15, 2022

2017), epibenthic (Becker et al. 2019), and demersal (Gallaway et al. 1981) fish species. Benthic invertebrates (Perkol-Finkel and Benayahu 2005) and even microorganism communities (Guo et al. 2021) are also influenced. The deployment of AR modules affects resident and migratory species by changing the topography and habitat, which influences how species aggregate and interact (Smith et al. 2017). In addition to providing feeding opportunities (Lindquist et al. 1994), ARs also provide shelter and protection for species and they attract organisms that have a preference for complex benthic structure (Hixon and Beets 1989). These responses triggered by ARs are often highly species specific and are sometimes specific to stages or sizes within a species (Foster et al. 1994).

Deciding the number and layout (connectivity) when deploying ARs is often focused on a few key species (Foster et al. 1994; Clark and Edwards 1999), even though ARs affect a wide diversity of species. Viewing the effects of ARs for the complex and diverse epibenthic multi-species ecosystem (Ardizzone et al. 1989; Sánchez-Jerez and Ramos-Esplá 2000) would help to inform management about likely responses (e.g., life history types, community) beyond the responses of a few focal or dominant species (Wang et al. 2015; Chen et al. 2019). Including the responses of the many species affected would allow for anticipating the full effects of ARs (Smith et al. 2011).

A challenge, therefore, is how to capture the responses of the many possibly affected species with a manageable and interpretable set of indicators. One approach is to develop distribution models (habitat–abundance) for each of the species. For example, single-species distribution models can be fitted based on generalized linear models (GLMs; McCullagh 1989) or generalized additive models (GAMs; Hastie and Tibshirani 1986). In addition to the difficulties in fitting so many models, interpreting and communicating the predicted responses to changes in habitat (due to ARs) are cumbersome (Hui et al. 2013). An approach taken here is to use classification methods to define species groups (archetypes) based on their similar responses to environmental variables and then to assess AR effects at the archetype level.

Some ARs are deployed adjacent to natural reefs, coral reefs, and abandoned oil platforms or are combined into AR structures (Coll et al. 1998; Ushiama et al. 2016; Lima et al. 2019; Schutter et al. 2019); these deployments produce complicated changes in substrate and other habitat-related variables. Effects of some variables, such as water quality (Godoy et al. 2002), occur on temporal and spatial scales that do not naturally align with the broader scales of interest (seasonal, habitat areas utilized) of species responses. When groups of species are the response variables, other factors related to AR effects also become complicated, such as how distances between AR modules affect the exchange (connectivity) of organisms (Smith et al. 2017). Furthermore, biological processes, such as predation, competition for shelters, preference for habitats, and mutualism (Zhang et al. 2018a), are further complicated by response variables that encompass multiple species (Pollock et al. 2014). A key becomes determining how to group species (e.g., archetypes) to ensure tolerable within-group variability and ecologically sound relationships with habitat and environmental variables while also providing useful information that captures the diversity of species responses.

The Bohai Strait and associated Bohai and Yellow seas constitute an important marine ecosystem that has relatively high flow exchange and supports feeding grounds and a passage corridor for fish migration (Guan et al. 2020). Recent investigations have reported a declining trend in multiple fishery stocks (Barman et al. 2020). As part of efforts to offset these declines, ARs were deployed to boost species productivity (Einbinder et al. 2006; Wu et al. 2016; Wang et al. 2019). Subsequently, rockfish species (such as Korean Rockfish *Sebastes schlegeli* and Fat Greenling *Hexagrammos otakii*) increased, at least partly due to ARs, and became dominant. The Asian paddle crab *Charybdis japonica* and rockfish species are economically important in the local area, followed by other reef-associated echinoderms (e.g., Japanese sea cucumber *Stichopus japonicus*), crustaceans (e.g., Pacific oyster *Crassostrea gigas*), and gastropods (e.g., veined rapa whelk *Rapana venosa*; Barman et al. 2020).

In this study, we used field monitoring data at a location in the south-central Bohai Strait with deployed ARs to identify archetypes and then used the fitted models to predict archetype responses to changes in habitat, including the presence of ARs. We first used statistical models to group epibenthic species associated with ARs by shared species–environment relationships into various species archetypes (SAs). The models were tested using field data and by comparing the fitted models to results from other machine-learning methods that use the species co-occurrence (without environmental variables) patterns. Our fitted models were then used to predict the occurrence probabilities of archetypes under different conditions of environmental factors. Our methods and analysis complement single-species analyses and can be used to inform management and others about the full range of organism responses to be expected from the deployment of ARs. Analyses of responses to ARs at the archetype level (and higher levels) enable the inclusion of many species in the analysis as an interpretable number of groups but also complicate the relationships of species to environmental and habitat variables because the results are no longer at the individual species level.

METHODS

Study area.— The study region is located in the south-central Bohai Strait and consists of a centrally located rocky reef with peripheral gravel and mud substrate; water depth varies from 8 to 31 m. Twenty-four AR modules, each a single 7.1- × 7.1- × 3.4-m (length × width × height) concrete structure, were deployed in the center of the study area in six clusters of four ARs each. The ARs within each cluster were about 10 m apart, and the clusters were deployed in a rough circle (black rectangle in Figure 1). The ARs were deployed in June 2017 about 500 m northwest of Xiaozhushan Island (38°1'45"N, 120°51'56"E). We divided the study area into three strata defined as concentric circles (radii of 200, 400, and 600 m) centered at the AR deployment location (Figure 1).

Sampling design and data collection.— Fourteen surveys were conducted using traps and visual methods from June 2017 to August 2020 that included sampling within each season (Table S.1 available in the Supplement separately online). The first 13 surveys were used for model fitting, and the final survey was reserved for model validation. For each survey, trapping occurred at 0–9 sites and visual sampling occurred at 0–11 sites (Table S.1). This resulted in a total (over all surveys) of 88 sites sampled by trapping and 71 sites sampled by visual census (Figure 2). We used a stratified random sampling design to select sites for each sampling event. Roughly equal numbers of sites were selected from each stratum for each survey when the sampling was viewed in total. The southeast region of the study area was not accessible for sampling.

Accordion traps and underwater visual census were used to catch nektonic and resident epibenthic species, including fish, crustaceans, cephalopods, gastropods, echinoderms, and mollusks. Each trap consisted of three cages in a series for a total length of 30 m, and the trap was deployed at each site for 48 h without bait. The catches from each trap were collected for species identification, enumeration, and weight measurement. For the visual census, we used the belt transect method (Bortone et al. 1986) and conducted a timed 20-min transect at each sampling site. Each transect was filmed by using a GoPro Hero 4, and the footage was reviewed in the laboratory to report the numbers observed by species. Species identification from underwater video was performed by three people: one individual conducted species identification of the whole video, while the other two people processed randomly selected video segments (10% of the length of the whole video). Species identification results were compared among the video analysts for the common segments, and

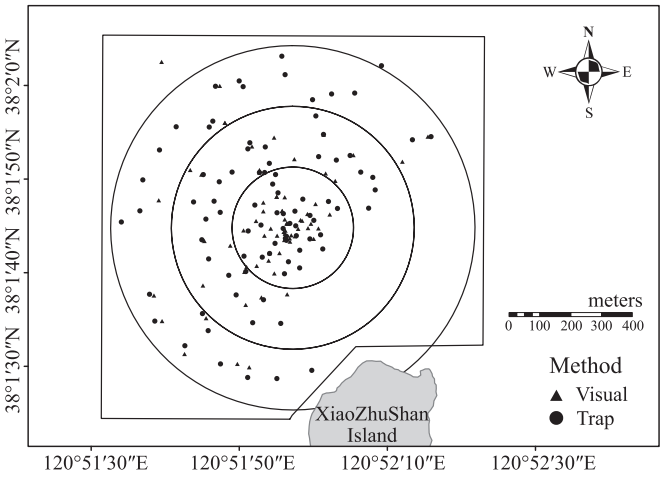

FIGURE 2. Distribution of sampling sites, cumulatively over all 14 surveys, for the trapping and visual census.

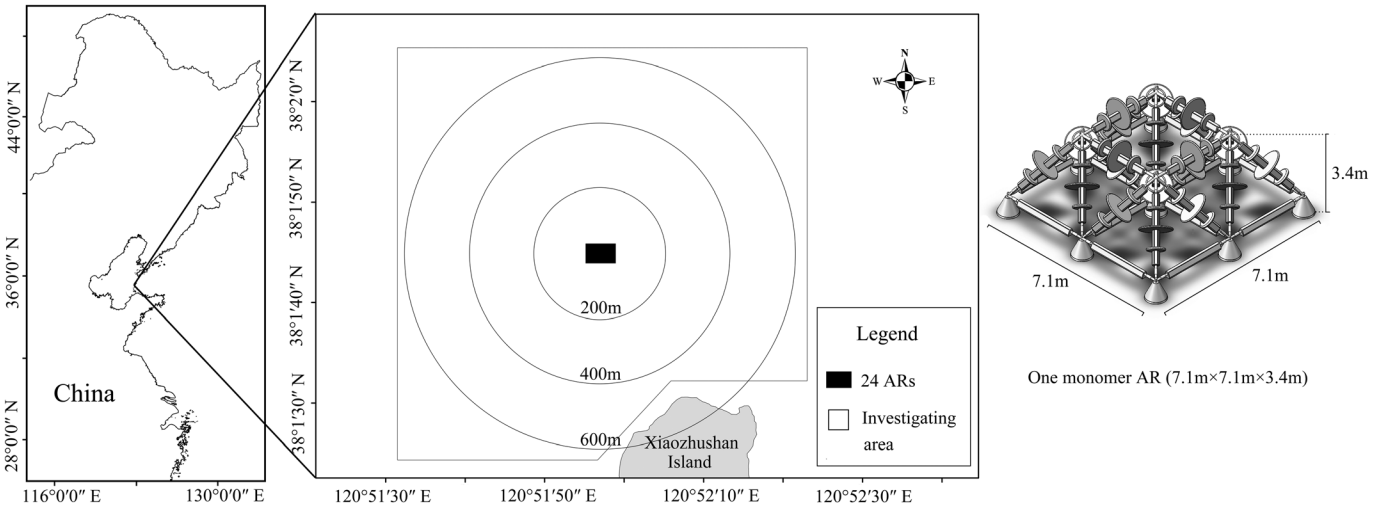

FIGURE 1. Study location and the local area surrounding the 24 artificial reefs (ARs) deployed in the Bohai Sea, China. A single AR (monomer) is shown on the right.

the entire video was reanalyzed until there were no differences (at least at the family level for some species) among the three individuals.

Fifteen explanatory variables were determined for each trap and visual sample (Table 1). Some environmental variables were collected at each site as part of the surveys. Temporally varying temperature (°C), bottom dissolved oxygen concentration (DO; mg/L), salinity (‰), and pH were measured at each site by using a YSI Pro Plus multiparameter water quality meter. Bottom water was sampled with a Plexiglas water collector at each site, and samples were transported to the laboratory to measure the chlorophyll-*a* concentration (mg/L); water transparency (m) was measured with a Secchi disk. Depth (m) was measured at each sampling site by a sonar lattice fish detector, and values were then assigned to each of 14,600 cells (10×10 m) that covered the entire study area by using inverse distance weight (IDW; Blanco et al. 2013) interpolation (Figure S.1 available in the Supplement separately online).

Bottom type was a categorical variable estimated by information on substrate from visual surveys that were distinct from the trapping and visual census surveys of organisms. Bottom type was scored into five categories using values of 0, 5, 20, 50, and 100 for mud, gravel, rubble, boulder, and AR (Mellin et al. 2007), respectively (Figure S.2). Bottom type was also assigned to each cell for the entire study region by using IDW interpolation of the scores observed at specific locations during June 2017–May 2020 as determined by the 63 underwater video sites (Figure 3). Video was processed by evaluating the bottom type at a site on frames every 5 s; all scores were combined for the interpolation. Interpolation was based on estimating bottom type averaged values, with the five classes treated as a continuous variable. Thus, unobserved cells that used nearby observed values would receive decimal values (e.g., 12.5). The exception was that boulder (100) was assumed to have a lower value of 99.9 to minimize its effect on the interpolation.

TABLE 1. Abbreviations of all environmental variables used in this study. The variables included in the species archetype model based on the stepwise identification of the final model with the lowest Bayesian information criterion and a variance inflation factor less than 6 are shown in bold. Temporally varying variables (abbreviations marked with an asterisk) were discrete samples taken at each survey.

Environmental variable	Abbreviation
Chlorophyll *a* (mg/L)	Chla*
Temperature (°C)	**Temp***
Dissolved oxygen (mg/L)	**DO***
Salinity (‰)	Sal*
Depth (m)	**Depth***
Transparency	Trans*
pH	pH*
Sampling method	**method**
Bottom type score	**BotType**
Duration of deployment of artificial reefs (months)	**Time**
Distance to the nearest mud (m)	dis.1
Distance to the nearest gravel (m)	**dis.2**
Distance to the nearest rubble (m)	dis.3
Distance to the nearest boulder (m)	dis.4
Distance to the nearest artificial reef (m)	**dis.5**

The remaining explanatory variables were determined from the survey details or derived from the habitat score map of the study area. Survey-based variables included a binary variable for sampling method (trap or visual) and a duration variable that was the number of months from AR deployment to the survey date. Bottom type was used to estimate the distances from the survey location to the nearest mud, gravel, rubble, boulder, and AR. These distances were determined based on the distance to the center of the nearest surrounding cell that was of the desired type (Figure S.1).

Community and dominant species.— The Shannon–Wiener biodiversity index was used as a measure of the complexity of the community (Külköylüoğlu et al. 2012; Adie et al. 2013). To minimize the effects of rare species, the species with a frequency of occurrence lower than 5% at sites were excluded from all further analyses. For trap and visual data, Pinkas' index of relative importance (IRI; Pinkas et al. 1971) was calculated to select dominant species at each site over the 13 surveys from June 2017 to May 2020. Scatterplots of the biodiversity index versus the bottom type score were generated for each sampling method (Figure 4). We used bottom type because it is known to be an important variable affecting species distributions and it is fixed through time (Sánchez-Jerez et al. 2002; Mellin et al. 2007). A locally estimated scatterplot smoother was then overlaid on each plot to identify possible relationships with habitat type. Plots were created while treating trap and visual census surveys separately (Table 2).

Species archetypes with shared environmental responses.— We classified species into archetypes based on shared responses to our explanatory variables using both surveys combined into presence/absence responses (Table 2) with the regression-based species archetype model (SAM; Dunstan et al. 2011). The SAM method has been utilized to describe cohesive environmental responses of herbaceous and woody plant species in the coastal plain (Silva and Souza 2018), detect community-level groupings (Leaper et al. 2014), and predict the composition of polychaete assemblages (Galanidi et al. 2016). The SAM is based on a single logistic GLM. One or many species with similar ecological tolerances are represented by the archetype GLMs derived from a single finite mixture model

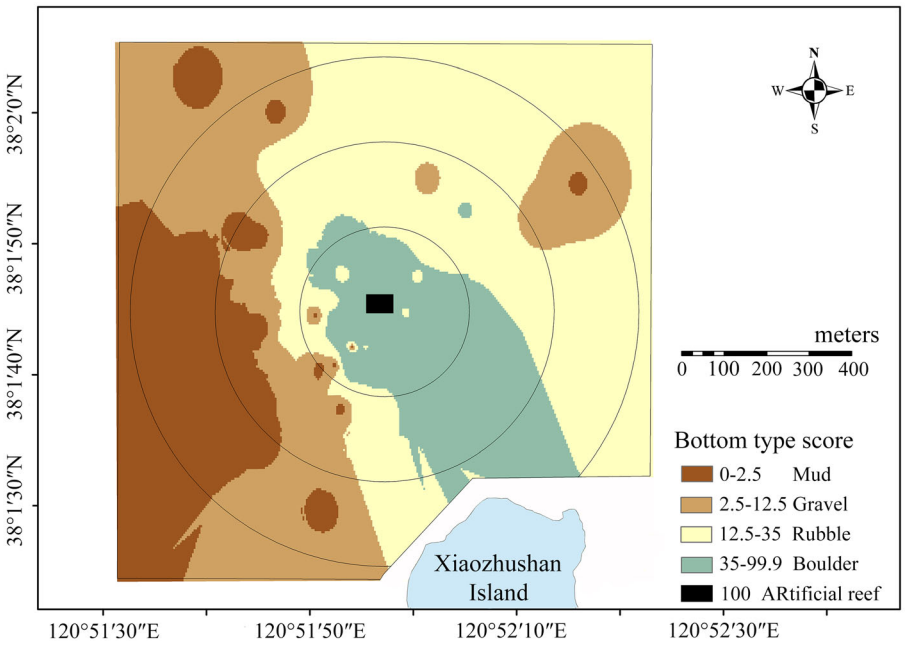

FIGURE 3. Estimated spatial map of bottom type scores. The interpolation treated the categorical bottom types as continuous variables, and the values for cells were then re-categorized into one of the five types by using the ranges shown in the legend.

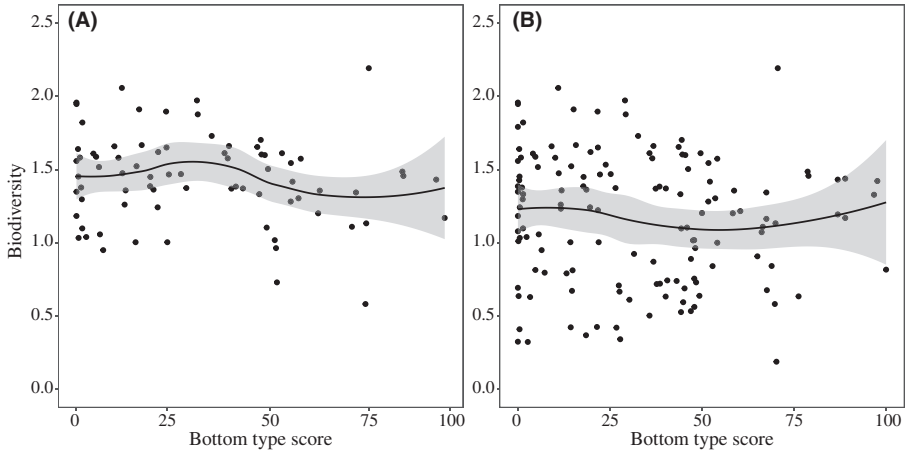

FIGURE 4. Plots of species biodiversity versus bottom type score for the **(A)** trapping and **(B)** visual sampling methods. Black dots are the sampling observations. The solid line through the data is a locally estimated scatterplot smoother; the shaded area is the 95% confidence interval of the smoother.

(Murillo et al. 2018). In our analysis, collinear variables were removed if the variance inflation factor (Lawesson 2009) exceeded a value of 6 (Zuur et al. 2010).

Estimation of the SAM was done using a stepwise approach and the Bayesian information criterion (BIC; Schwartz 1978). Models were applied using all of the explanatory variables, and the desired number of groups was specified as a progression from 1 to 20 archetypes. The $\Delta\mathrm{BIC}(i)$ for the ith model was calculated as $\mathrm{BIC}(i) - \mathrm{BIC}(i+1)$. The version (number of archetypes and combination of explanatory variables) with the lowest BIC value was selected.

Two additional considerations were used to confirm the validity of the archetypes identified based on BIC with the SAMs. First, we applied the approach of Dunstan et al. (2011), in which the minimum probability (π), which is the contribution of the specific proportions of each species to an archetype, should be higher than the probability of a single species randomly belonging to an archetype ($1/S$, where S is the number of species in the archetype). The

TABLE 2. Summary of the analyses used in this study, the treatment of the trap and visual census data, and the tables and figures used to display the results for each analysis.

Analysis item	Treatment of trap and visual data	Results	Tables and figures
Community and dominant species using index of relative importance (IRI)	Separate; continuous	Scatterplots of biodiversity and abundance for representative dominant species from each archetype versus bottom type scores	Tables S.2, S.3; Figures 4, 8
Fitting the species archetype model (SAM)	Combined; presence/absence	Identification of six archetypes and predicted maps of occurrence probability and SEs based on annual and season-specific averages of environmental variables	Tables 3, S.4, S.5; Figures 5, 6, 7, S.3–S.7
Using the SAM to predict occurrence probabilities	Combined; presence/absence	Marginal responses to each environmental variable with others set to their minimum, mean, or maximum values	Tables 3, 4; Figure 10
Fitting ISOPAM	Combined; presence/absence	Used ISOPAM to estimate the fidelity of species in archetypes from the SAM; spatial distribution of sampling sites categorized by their group (ISOPAM) versus archetype (SAM)	Tables 3, S.8; Figure 9
Using the SAM to predict occurrence probabilities	Combined; presence/absence	Predicted occurrence probabilities with all environmental variables set to their minimum, mean, maximum, or optimal values	Figure 11
SAM validation	Combined; presence/absence	Comparison of mean square error with that of the final survey (August 2020)	Figure 12

SAM assigned the probabilities of membership of each species to each archetype. In the present study, we set a threshold of 0.99 for each species to identify species that were strongly affiliated to the particular archetype (Foster et al. 2015). Secondly, we used relative standard error (RSE) to reflect the importance of each environmental variable, where RSE is the absolute value of the SE of a parameter value multiplied by 100 and divided by the value of its estimated coefficient. A high value of RSE indicates that the environmental variable has less importance. We applied both considerations to the set of archetypes selected from the stepwise approach. The analysis was conducted using the SpeciesMix package in R.

Based on the species composition of each archetype, an economically important species from each archetype (highest IRI value among important species) was selected as the representative dominant species. Scatterplots of the relationship between the abundance of representative species and the bottom type score were created separately for trapping and visual survey methods with a locally estimated scatterplot smoother overlaid.

Species classification based on co-occurrence patterns.—An alternative classification method to SAM was also applied to the survey data to examine the degree of consistency in SAM assignment of species to archetypes. Whereas SAM used the environmental variables, the isometric feature mapping and partitioning around medoids (ISOPAM) approach depended only on the species composition observed at sites in the surveys. The ISOPAM method uses nonlinear dimensionality reduction and parameter optimization based on species occurrence (Schmidtlein et al. 2010), which was applied here to the species from the combined trapping and visual census surveys (Table 2). We used the value of the phi (φ) coefficient and its significance ($\alpha = 0.01$) to evaluate the results of the ISOPAM classifications. Phi ranges from -1 to 1 and measures the degree to which a species belongs to a specific group (Tichy and Chytry 2006). A φ value of 0.37 was used to distinguish species with low fidelity ($\varphi < 0.37$) or high fidelity ($\varphi \geq 0.37$) to their group. The analysis used the package isopam in R.

The results from ISOPAM were used in two ways to check the species assignments to archetypes according to SAM (Table 2). For each species assigned to each archetype by SAM, we determined whether ISOPAM estimated that species to have high fidelity to the archetype (Murillo et al. 2018). An ordered synoptic table was made by combining the results of SAM with the fidelity values of member species from ISOPAM. The results compared how species were grouped based on similar responses to environmental variables with their likelihood of belonging (i.e., fidelity) based on the species co-occurrence patterns

(Murillo et al. 2018). We also plotted the distribution of sampling sites for surveys coded by archetype and alternatively coded by the co-occurrence groups from ISOPAM.

Occurrence probabilities of archetypes.—We used the fitted SAM to generate season-specific and annual occurrence probability maps for the study area (10- × 10-m cells) by summarizing the environmental explanatory variables and using them as inputs to the SAM (Table 2). For temporally varying variables, seasonal and annual averages (i.e., temperature and DO) were calculated corresponding to the specific months of each of the 13 surveys (June 2017–May 2020; Table S.1). The cell-specific spatial variables (i.e., bottom type score, depth, distance to the nearest gravel, and distance to the nearest AR) were generated from the field data, and we utilized IDW interpolation to assign values of selected fitted environmental variables to each grid cell. Based on fixing the locations of the ARs (to generate distances to the nearest AR and gravel) and setting the duration of AR deployment to 35 months (longest value), occurrence probability maps were separately predicted for the trapping and visual census methods. To explore the influence of season on the species assemblage, we used Venn diagrams (by season) to display the differences in species compositions being selected for inclusion in the SAM.

The sensitivity of archetypes to changes in environmental variables was then assessed by determining how their occurrence probabilities changed in response to different assumed values for combinations of explanatory variables. We used two measurements of fixing values of environmental variables. First, marginal effects plots were separately generated for the archetypes for each environmental variable with all other variables set to their minimum, mean, and maximum values. Secondly, we fixed all selected environmental variables at their minimum, mean, maximum, and optimal values. Optimal values across all environmental variables for each archetype were determined by using the maximum value of positive coefficients and the minimum value for negative coefficients.

Model validation.—Validation of the SAM archetypes was done by comparing predicted and observed values for the August 2020 (16 sites) survey, which was not used in model fitting. Using environmental variables measured at each site, the SAM was used to generate the occurrence probabilities of the six SAs for each sampling site. Observed values were generated using trap and visual census data combined and were converted to presence/absence (Table 2). If any species in an archetype was present in the data, then that archetype was assigned an occurrence probability of 1.0 for that site; otherwise, it was assigned a zero. Mean square error (MSE) was computed as differences in the observed and predicted occurrence probabilities squared and then summed over the 16 sites for each of the six archetypes and divided by 16 (i.e., the number of sites). Predicted occurrence probabilities from the fitted SAM based on field data (June 2017–May 2020; used for model fitting) were used to generate MSE values for each archetype as a basis of comparison for the MSE values from the validation survey.

RESULTS

Sixty epibenthic species, including fish, crustaceans, echinoderms, cephalopods, mollusks, and gastropods, were sampled by traps, and 34 epibenthic species (including bivalves as well) were sampled by visual census.

Community and Dominant Species

For data from the trap method, four species were identified as dominant (IRI > 1,000). *Charybdis japonica*, Korean Rockfish, Fat Greenling, and blue bat star *Asterina pectinifera* had the highest IRI values (Table S.2). For visual census data, which included reporting of abundance, IRI based on the percentage of abundance identified six species as dominant (i.e., IRI > 100), with *A. pectinifera* accounting for 62% of the total abundance. The remaining dominant species were the Chameleon Goby *Tridentiger trigonocephalus*, *C. japonica*, Japanese seastar *Asterias amurensis*, Fat Greenling, and Korean Rockfish (Table S.3). Biodiversity of trapping and visual methods did not display any clear patterns across bottom substrate type (Figure 4).

Species Groups and Responses to Environment

Six archetypes were identified, which involved 23 species (Table 3), with this particular model having the lowest BIC value and positioned in the stepwise sequence just prior to a large increase in ΔBIC (Figure 5A, B). The selected six-archetype model used temperature, DO, depth, sampling method, bottom type score, time since AR placement, and distances to the nearest gravel (dis.2) and the nearest AR (dis.5) as important explanatory variables (Table 1). This subset of variables also did not have collinear effects, and the corresponding minimum π was higher than $1/S$ (Figure 5C). The coefficients, SEs, and RSEs of the six archetype GLMs are shown in Table S.4, and the species composition and membership probabilities are shown in Table S.5. Membership probabilities were mostly higher than 0.99.

Species archetypes included two or more species except for SA1, and SA5 contained nine species (Table S.5). Species archetype 4 included the same four dominant species between the trap and visual methods (Tables S.2, S.3). Spatial distributions of the sampling sites according to their archetype displayed similarity across archetypes and a distinct pattern of sites being aggregated in the proximity of the ARs (Figure 6); the exception was SA5, which showed an inverse pattern due to its member species'

TABLE 3. Ordered synoptic table made by combined grouping results of the species archetype model (SAM) and the ISOPAM method associated with the highest fidelity of the species (represented by φ) and the responding degree of each species archetype (SA) for each environmental variable. The threshold of the φ value was used to distinguish species that could be identified into an ISOPAM group (I–IVb; $\varphi \geq 0.37$) and those that could not be adequately identified into a group ($\varphi < 0.37$). The range of each variable is shown under the corresponding name (abbreviations for variables are defined in Table 1). Arrow direction is based on the coefficients in the SAM (up arrow [↑] = positive response for the variable; down arrow [↓] = negative response for the variable), and the number of arrows represents the importance of the variable depending on the relative standard error (RSE; three arrows: RSE ≤ 50; two arrows: 50 < RSE ≤ 100; one arrow: 100 < RSE ≤ 150; dash [–]: RSE > 150).

Taxon	Species name	SA	ISOPAM φ value	Temp (6.0–25.0°C)	DO (6.0–13.1 mg/L)	Depth (9.8–32.0 m)	BotType (0–100)	Method (trap or visual)	Time (0–35 months)	dis.2 (1.0–190.9 m)	dis.5 (2.4–567.5 m)
Gastropoda	Veined rapa whelk *Rapana venosa*	SA1	<0.37	↑	↑	↓↓	↑↑↑	↑	–	↓↓↓	↑↑
Echinodermata	Japanese sea cucumber *Stichopus japonicus*	SA2	IVb: 0.74	↓↓	↑	↑↑	–	↑↑↑	↓↓	↑↑↑	↓↓
Echinodermata	Sea urchin *Strongylocentrotus nudus*	SA2	<0.37								
Teleostei	Goby *Stonogobiops pentafasciata*	SA2	<0.37								
Echinodermata	Japanese seastar *Asterias amurensis*	SA3	IVb: 0.68	–	–	–	–	↑↑↑	↓↓	↑↑	↓↓
Teleostei	Chameleon Goby *Tridentiger trigonocephalus*	SA3	IVa: 0.73								
Teleostei	Fat Greenling *Hexagrammos otakii*	SA4	II: 0.42	↑↑↑	↑↑	↑↑↑	↑↑↑	↓↓↓	↑↑↑	↑↑	↓↓
Teleostei	Korean Rockfish *Sebastes schlegeli*	SA4	II: 0.42								
Echinodermata	Blue bat star *Asterina pectinifera*	SA4	<0.37								
Crustacea	Asian paddle crab *Charybdis japonica*	SA4	<0.37								
Crustacea	Japanese mantis shrimp *Oratosquilla oratoria*	SA5	I: 0.57	↓↓↓	↓↓↓	–	↓↓	↓↓↓	↓↓↓	↓↓↓	↑↑↑
Crustacea	Japanese snapping shrimp *Alpheus japonicus*	SA5	I: 0.53								
Cephalopoda	Whiparm octopus *Octopus variabilis*	SA5	I: 0.43								
Crustacea	Gladiator prawn *Palaemon ortmanni*	SA5	I: 0.42								
Teleostei	Goby *Amblychaeturichthys hexanema*	SA5	III: 0.64								
Teleostei	Branded Goby *Chaeturichthys stigmatias*	SA5	<0.37								

TABLE 3. Continued.

Taxon	Species name	SA	ISOPAM φ value	Temp (6.0–25.0°C)	DO (6.0–13.1 mg/L)	Depth (9.8–32.0 m)	BotType (0–100)	Method (trap or visual)	Time (0–35 months)	dis.2 (1.0–190.9 m)	dis.5 (2.4–567.5 m)
Crustacea	*Palaemon gravieri*	SA5	<0.37								
Teleostei	Fringed Blenny *Chirolophis japonicus*	SA5	<0.37								
Teleostei	Shokihaze Goby *Triaenopogon barbatus*	SA5	<0.37								
Teleostei	Marbled Flounder *Pseudopleuronectes yokohamae*	SA6	<0.37	↑↑	–	↑↑	–	↓↓↓	–	↑↑	↓↓↓
Teleostei	False Kelpfish *Sebastiscus marmoratus*	SA6	<0.37								
Teleostei	Rockfish *Sebastes hubbsi*	SA6	<0.37								
Teleostei	Black Scraper *Thamnaconus modestus*	SA6	<0.37								

preferences for mud and gravel. Temporally varying variables (temperature and DO) varied across the four seasons, but they did not show significant variation (i.e., SDs were small) within individual surveys (Table S.6). Occurrence probabilities and their SEs for the six archetypes, both seasonally (Figures S.3–S.6) and annually (Figure 7), showed similar results for SA1 and SA4–SA6 based on both the trap and visual census sampling methods. Species archetypes 2 and 3 had higher probabilities for visual census survey data than for trap data (Figure 7). Species archetype 4 was broadly distributed and exhibited high occurrence probability across the whole area, with the highest probabilities located near ARs and boulder substrate. Venn diagrams showed that there was no highly season-specific species and that most species (60.9%) occurred in all four seasons (Figure S.7). Apart from winter, 17.4% of species appeared in spring, summer, and autumn. All species were present in summer, and many species (6/23) in SA1, SA2, SA5, and SA6 were absent in winter (Table S.7). Member species belonging to SA3 and SA4 did not show seasonal differences.

Based on the IRI values for each species from the trapping and visual methods (Tables S.2, S.3), we defined *R. venosa*, *A. amurensis*, *C. japonica*, Japanese mantis shrimp *Oratosquilla oratoria*, and the rockfish *Sebastes hubbsi* as the representative dominant species for SA1, SA3, SA4, SA5, and SA6, respectively, via trapping. Limited sampling of the only species in SA2 with trapping prevented interpretation. *Rapana venosa*, *S. japonicus*, *A. amurensis*, *C. japonica*, the goby *Amblychaeturichthys hexanema*, and *S. hubbsi* were separately selected as representative dominant species for SA1–SA6 based on data from visual sampling. Trapping had limited effectiveness around ARs (bottom type score = 100; Figure 8A), while the more effective visual sampling observed fish that were associated with the complex habitat (bottom type score > 50; Figure 8B). When the two sampling methods were combined (Figure 8), *R. venosa* of SA1 showed high abundance on gravel, boulder, and AR substrates (bottom type score = 10, 50–100), and the abundance of *S. japonicus* from SA2 showed a sharp increase with boulder substrate, but observations were limited for gravel and mud types. *Charybdis japonica* and *S. hubbsi* represented SA4 and SA6, respectively, and showed increased abundance when the bottom type score was greater than 50. Trapping and visual data both showed that *O. oratoria* and *A. hexanema* of SA5 had higher abundances with mud and gravel substrates. Finally, *A. amurensis* of SA3 did not show a clear relationship between abundance and bottom type score.

Species classified into groups by ISOPAM were generally similar to the species in the archetypes (Table 3). The ISOPAM method identified five groups that involved 10 species (Table 3). Fidelity values estimated by ISOPAM (Table S.8) for the 23 species included in the SAM-based

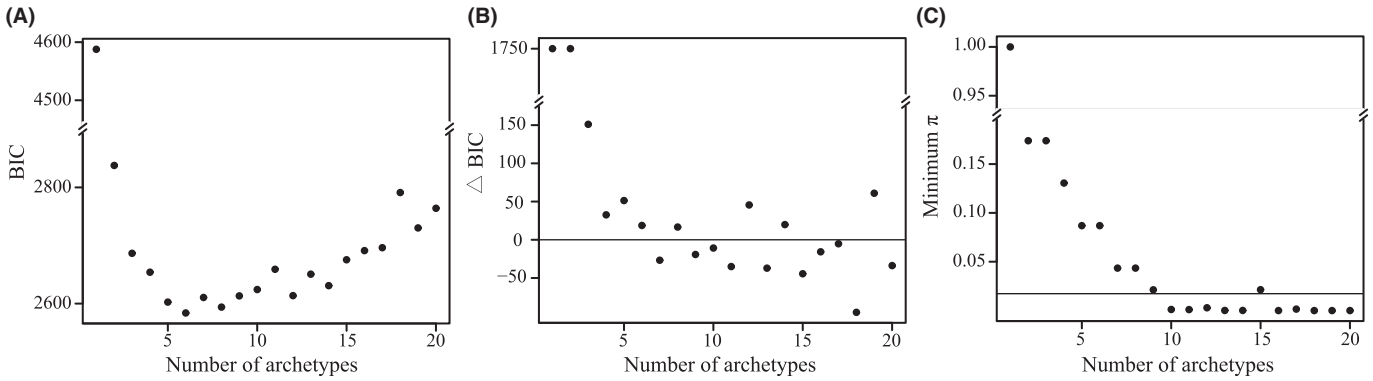

FIGURE 5. Values of **(A)** Bayesian information criterion (BIC), **(B)** ΔBIC (horizontal line indicates ΔBIC = 0), and **(C)** minimum probability π (defined in Methods; horizontal line indicates $1/S = 1/23$) for species archetype model selection in the stepwise process using 1–20 archetypes.

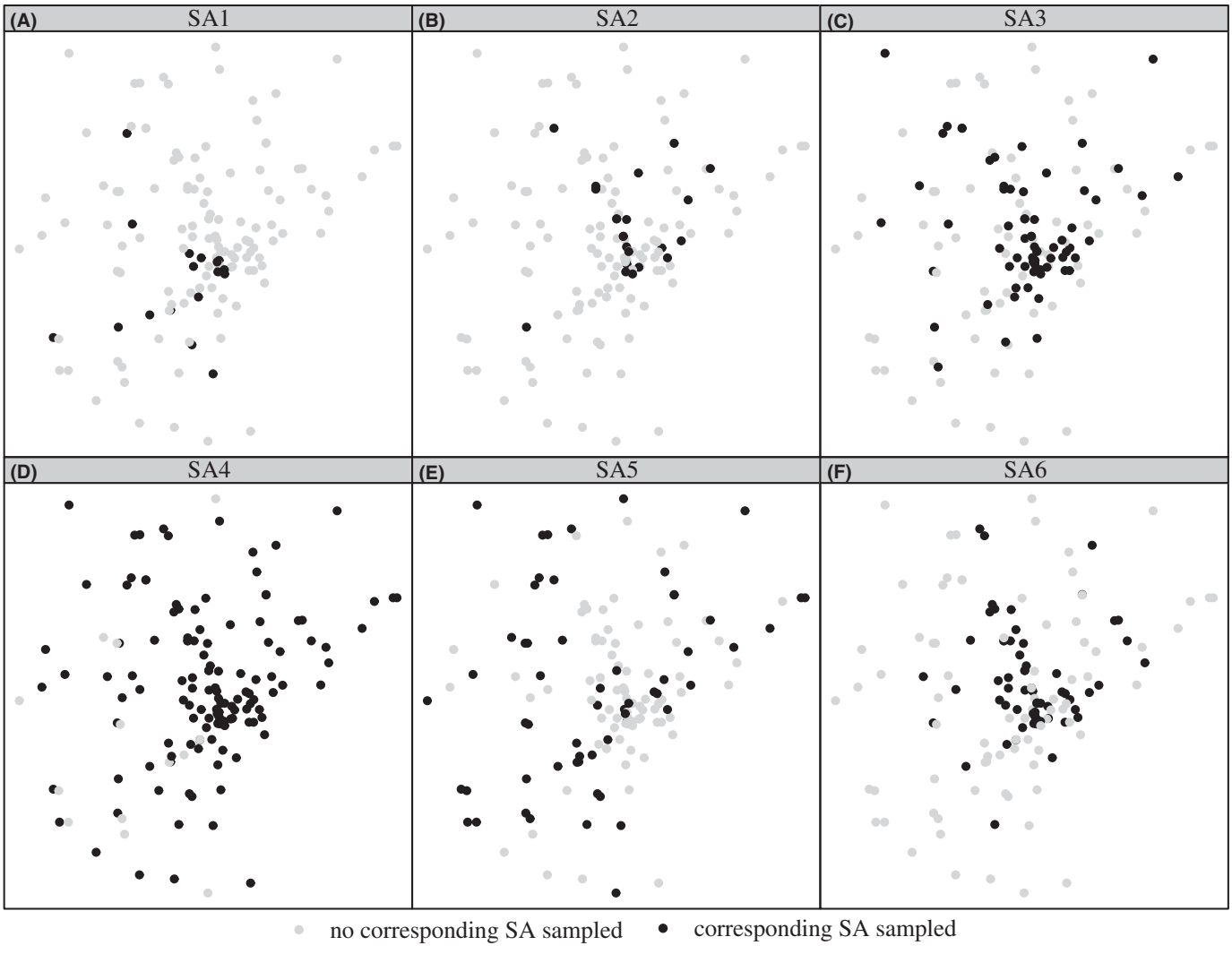

FIGURE 6. Distribution of sampling sites identified for each species archetype (SA; panels **A–F** refer to SA1–SA6).

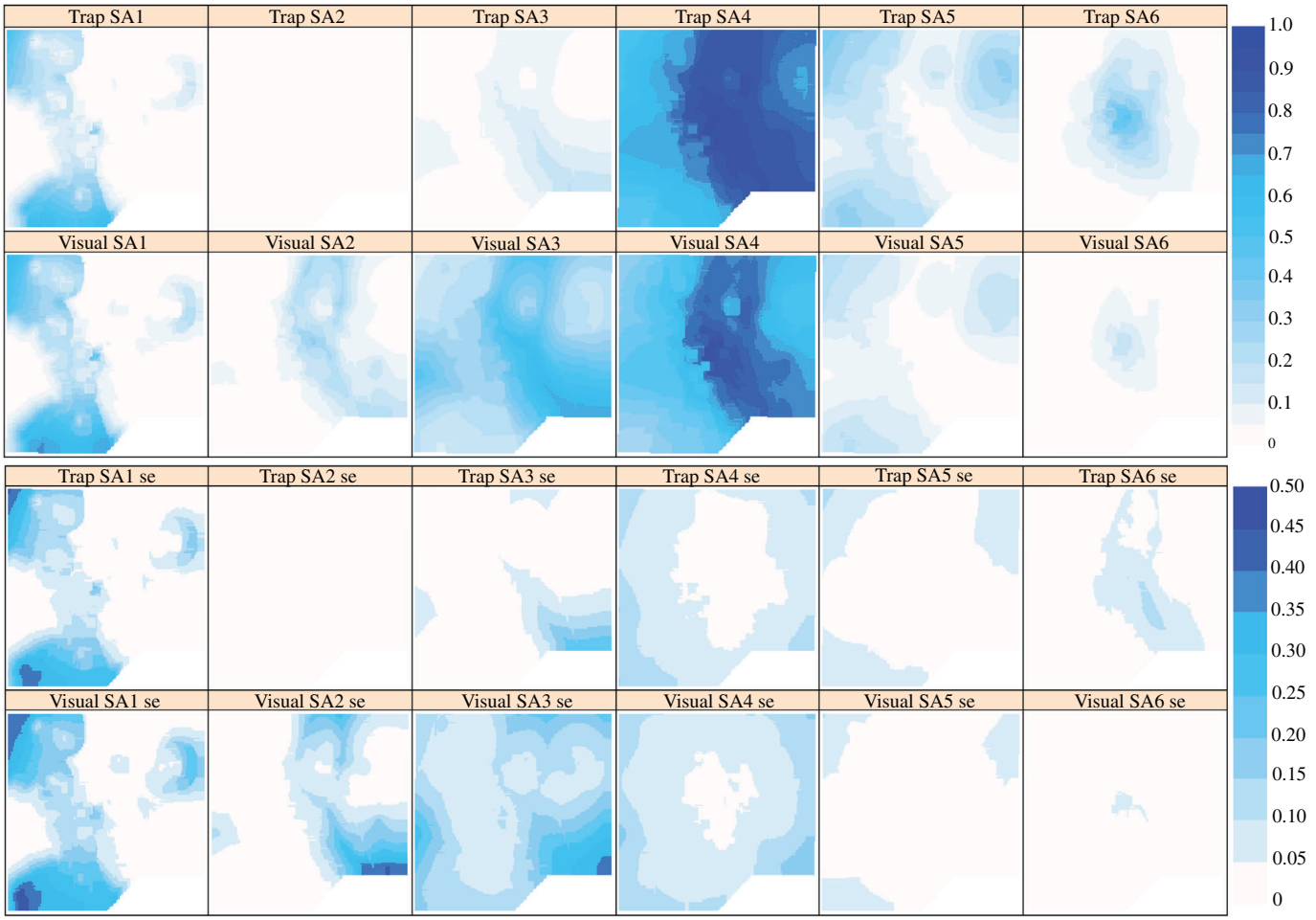

FIGURE 7. Spatial map of the predicted occurrence probabilities and SEs for each species archetype (SA1–SA6) for the trap and visual census methods based on annual averaged values of explanatory variables.

archetypes showed some correspondence. Species archetype 1 (one species) and SA6 (four species) had no species with high fidelities. One of three species in SA2, both species in SA3, and two of four species in SA4 had high fidelities; five of nine species in SA5 had high fidelities, but those species were from two different ISOPAM groups (four from group I and one from group III). Spatial distribution of sites affiliated with each group also displayed agreement between SAM and ISOPAM (Figure 9 versus Figure 6).

Occurrence probabilities of SAs responding to individual environmental variation showed generally monotonic relationships (Figure 10) and important differences among the archetypes (Table 3). Based on the summarized results (Tables 3, 4), SA1 represented a shallow-water (average depth = 9.8 m) archetype that preferred to distribute on AR substrate and also near gravel. Species archetype 2 was a reef-neighbor, visual census-dependent archetype that preferred cooler conditions (6.0°C). Species archetype 3 was also visual census dependent but was more general, as it showed little preference for specific substrate types. Species archetype 4 was a dominant archetype whose member species were distributed in deep waters (31.3 m) near ARs that were warmer (25.0°C), and their preferences gained strength with deployment (35 months). Species archetype 5 was a coldwater, soft-sediment type that differed greatly (almost inversely) from the other archetypes: SA5 preferred cool temperatures (6.0°C), relatively low DO (6.0 mg/L), flat substrate, and being some distance from the AR deployment. Finally, SA6 was a DO-independent, reef-neighbor archetype that preferred warmer (25.0°C), deep (31.3-m) waters and being close to ARs.

When all environmental variables were set at their minimum, mean, maximum, and optimal values, occurrence probabilities of the SAs showed different and wide-ranging responses (Figure 11). Species archetypes 1, 5, and 6 displayed decreasing probabilities from minimum to maximum values; occurrence probabilities of SA1 and SA6 remained very low (<0.2), with both archetypes from

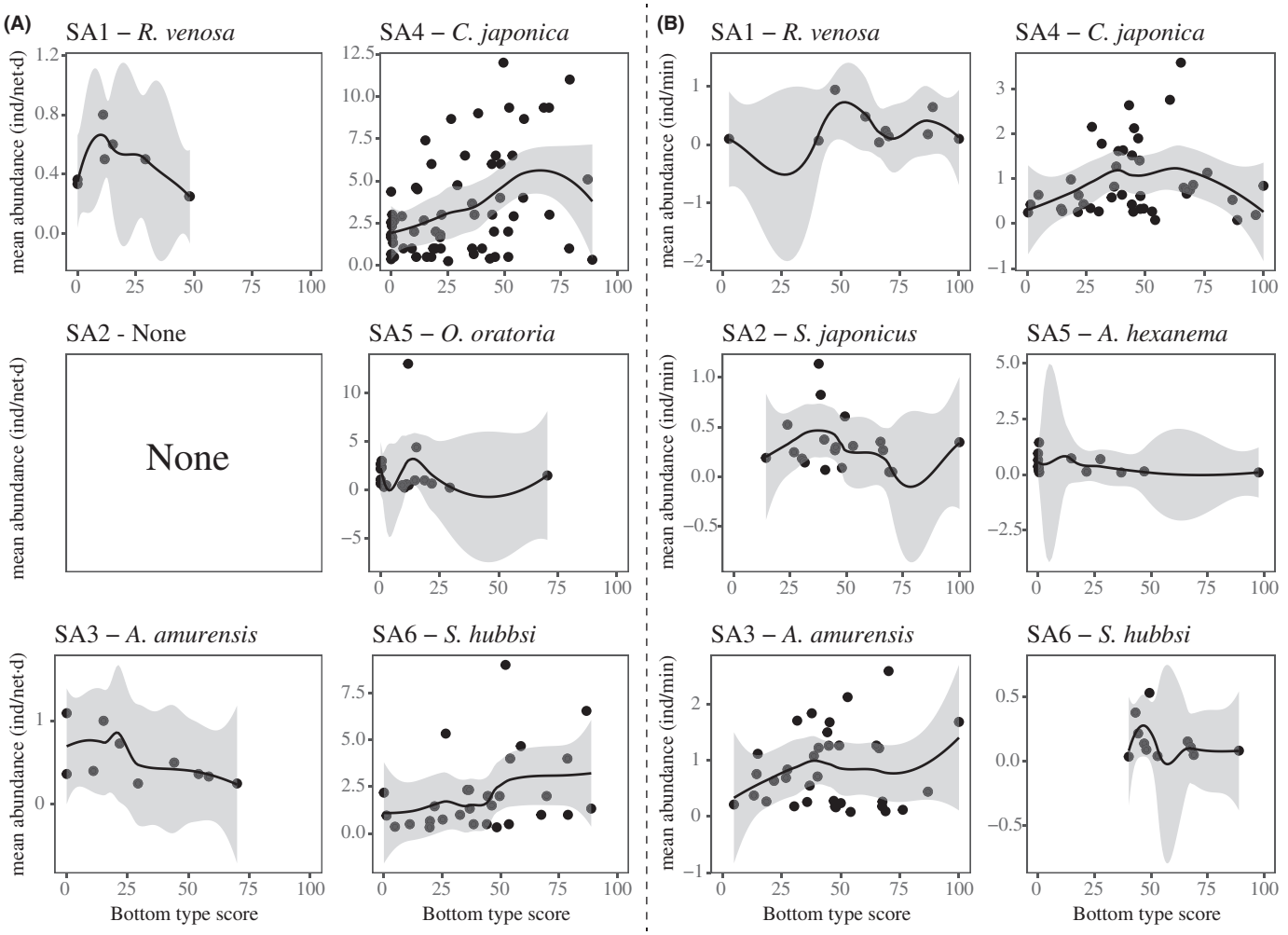

FIGURE 8. Plots of mean abundance versus bottom type score for the representative dominant species from each species archetype (SA) based on the **(A)** trapping method (individuals [ind]/net day) and **(B)** visual census method (ind/min). *Rapana venosa* (Gastropoda), *Asterias amurensis* (Echinodermata), *Charybdis japonica* (Crustacea), *Oratosquilla oratoria* (Crustacea), and *Sebastes hubbsi* (Teleostei) were selected as representative dominant species for SA1 and SA3–SA6 for the trapping method. *Rapana venosa*, *Stichopus japonicus* (Echinodermata), *A. amurensis*, *C. japonica*, *Amblychaeturichthys hexanema* (Teleostei), and *S. hubbsi* were selected as dominant species for SA1–SA6 for the visual method. The solid line through the data is a locally estimated scatterplot smoother; the shaded area is the 95% confidence interval of the smoother.

minimum to maximum having values lower than with average values (Figure 11A, F). For example, the occurrence probability of SA5 was 0.58 when all variables were set to their minimum values and then sharply decreased to 0.01 with all variables set at their maximum values (Figure 11E). The maximal potential values of occurrence probability for SA1, SA5, and SA6 were higher than 0.85, and SA1 approached 0.99 when all environmental variables were set to their optimal conditions. Species archetypes 2, 3, and 4 displayed increasing occurrence probabilities for variables set at the minimum to optimal values; SA2 showed the largest change of 0.01 (minimum) to 0.99 (optimal), followed by SA4 (from 0.15 to 0.99) and SA3 (from 0.11 to 0.76; Figure 11B–D).

Species Archetype Model Validation

The SAM performed equally well when challenged with data from the validation survey (August 2020) as compared to the results from being fitted to the earlier 13 surveys (Figure 12). The MSE values for the validation were similar except for the relatively high values (>0.4) for SA3 and SA5. Species archetype 4 had the lowest MSE value under validation.

DISCUSSION

The correspondence between the archetypes from SAM and the groupings and membership fidelities from ISOPAM shows that the relationships between 10 of 23

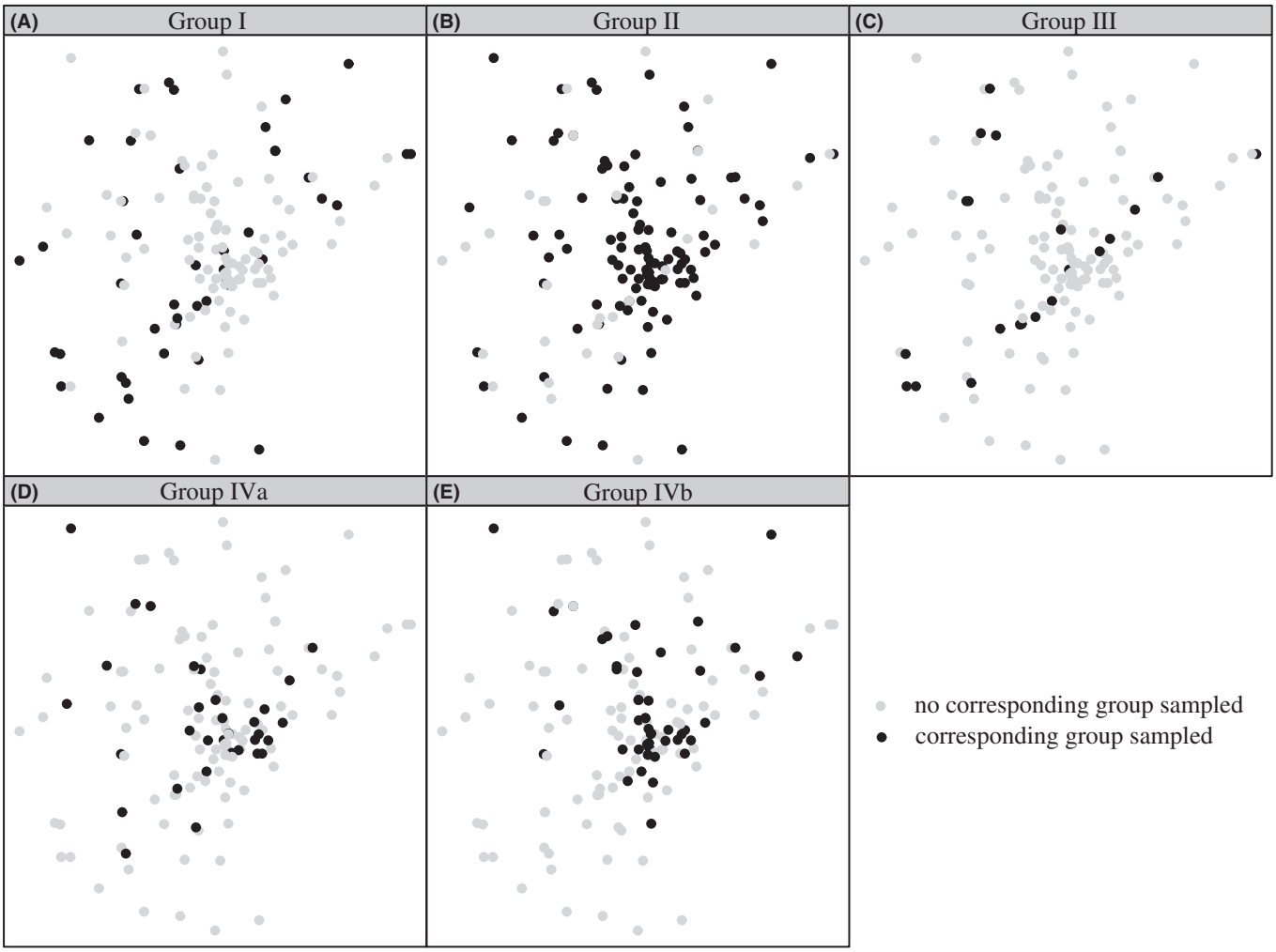

FIGURE 9. Distribution of sampling sites for each grouping identified by ISOPAM (panels **A–E** refer to groups I–IVb).

species' responses to environmental conditions are coupled to those 10 species' co-occurrence patterns. Both methods were applied to 23 of the 60 species because our filtering criterion required a frequency of occurrence at sites greater than 5%, which eliminated 37 relatively rare species from both analyses. Of those 10 species in common to SAM and ISOPAM, two of the four species that occurred in SA4 also occurred in ISOPAM group II, and four of the nine species occurring in SA5 also occurred in ISOPAM group I. However, the other 13 species assigned to SAM archetypes were not included in any of the ISOPAM groups. A possible explanation for the fewer species included in ISOPAM groups is that SAM used species–environment information, while ISOPAM used species co-occurrence.

The influence of season on the species compositions of the archetypes may be reflected by differences in the species with responses to temporally varying variables (i.e., temperature and DO). For example, species in SA6 showed a preference for warmer water and 50% of species were absent in winter. However, most of the species in our analysis are resident, habitat type dependent, or significantly affected by AR deployment, so simple relationships to temperature or DO (seasonally varying variables) are unlikely. Those species that showed a high dependence on temperature or DO (e.g., SA4) did so across all seasons. The similar seasonal distribution of occurrence probabilities for the six archetypes (Figures S.3–S.6) and no season-specific species (Figure S.7) may explain the relative lack of seasonality in the species and archetypes.

The biodiversity index did not show a clear dependence on the complexity of the habitat (i.e., mud, gravel, rubble, boulder, and AR), suggesting that species were using multiple habitats throughout the ARs and surrounding area. The deployment of ARs should not only focus on the assemblages of AR-oriented species but should also

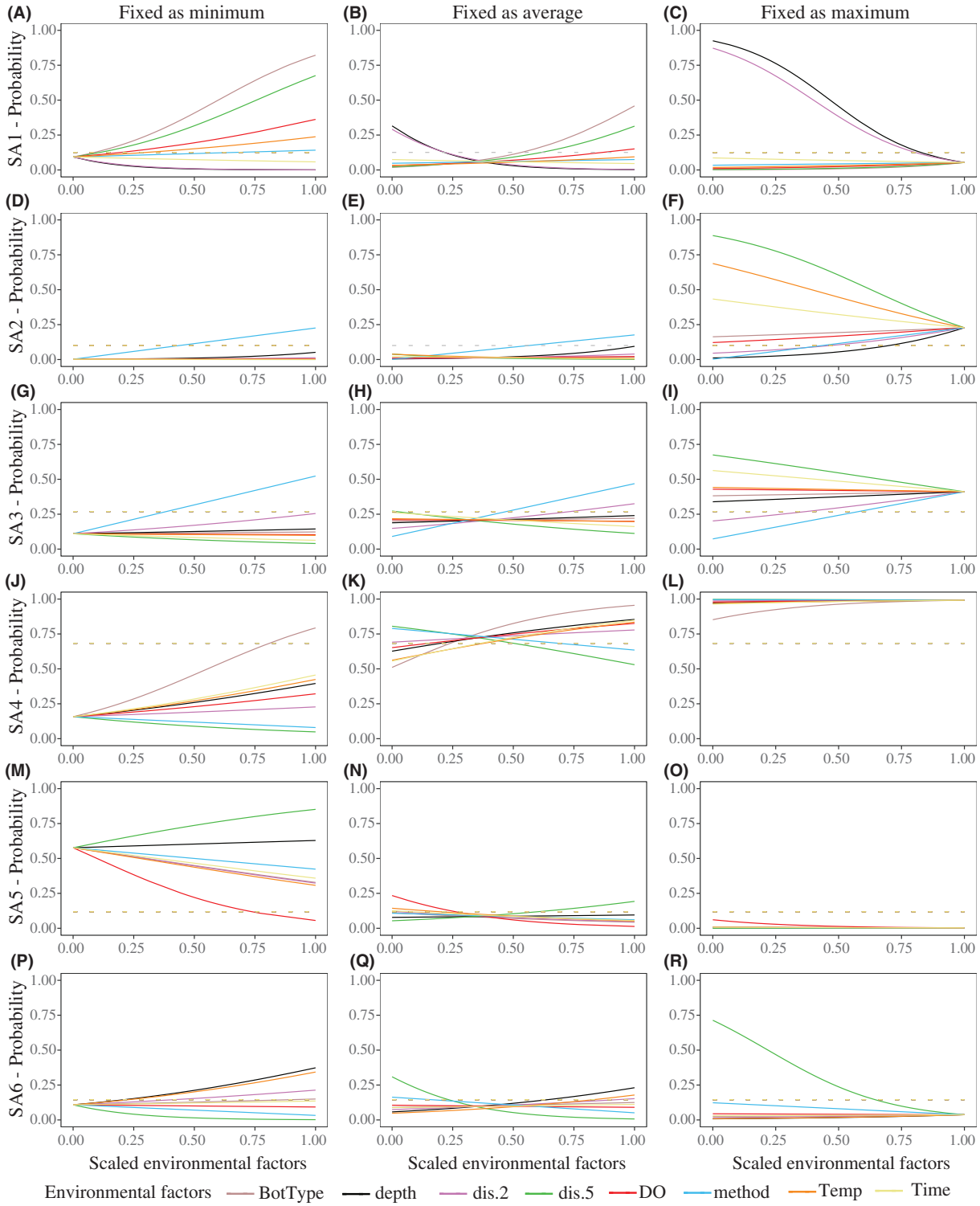

FIGURE 10. Marginal effect responses of species archetypes (SAs) to each environmental variable when all other variables were held constant at their respective minimum, mean, and maximum values (abbreviations for variables are defined in Table 1). The range of each environmental variable is scaled from 0 to 1 for the *x*-axis. Dashed lines represent the average of occurrence probabilities for the SAs identified by species archetype modeling: **(A)–(C)** SA1; **(D)–(F)** SA2; **(G)–(I)** SA3; **(J)–(L)** SA4; **(M)–(O)** SA5; and **(P)–(R)** SA6.

TABLE 4. Summary of the responses of each species archetype (SA) to the significant preferred environment (variables with a relative standard error < 50 and high sensitivity; abbreviations for variables are defined in Table 1; AR = artificial reef), related information of extreme sensitivity, original occurrence probability without any sensitivity assessment (Figure 10), and optimal occurrence probability (Figure 11). A dash (–) indicates that there is no related description for the item.

	Habitat		Hydrology		Sampling				
SA	Depth	Substrate	DO	Temp	Method	Duration of AR deployment	Extreme sensitivity	Original mean occurrence probability	Maximum occurrence probability
SA1	Shallow	Complex substrate but prone to gravel	–	–	–	–	Depth: 0.05–0.93 m at max	0.13	0.99
SA2	–	Near ARs	–	Cool	Visual census	–	Dist.5: 0.23–0.89 m at max	0.10	0.99
SA3	–	–	–	–	Visual census	–	Visual census: 0.11–0.52 at min	0.27	0.79
SA4	Deep	Complex substrate	–	Warm	–	Long time	BotType score: 0.16–79 at min	0.68	0.99
SA5	–	Soft, flat substrate and away from ARs	Low	Cold	Trap	Short time	DO: 0.06–0.58 mg/L at min	0.12	0.86
SA6	Deep	Near ARs	–	Warm	Trap	Short time	Dis.5: 0.04–0.71 m at max	0.15	0.86

consider other species, such as those in SA5 that prefer soft sediments (Butman 1987; Reeds et al. 2018).

Archetypes and Responses to Environmental Variables

For our marginal effects analyses and for the analyses in which all variables were set to minimum, mean, maximum, or optimal values, we used the full range of environmental values observed in the sampling. This illuminated the response potential of the archetypes to local environmental conditions. Relatively low values of occurrence probabilities under optimal conditions (Figure 11; e.g., maximum of 0.76 for SA3) implied that the probability of distribution of SA3 was relatively low throughout the study area. Species archetype 3 had very high deviance values (high RSE in Table S.4), indicating that the influence of local environmental variables was small. It is possible that important environmental variables were not included or that other sampling methods would have increased the occurrence probabilities. For example, the influential environmental conditions for SA6 of warm and low-DO water may occur by seasonal stratification and eutrophication-related summer DO depletion in the Bohai Sea (Zhai et al. 2019), which the monitoring data reported here were not designed to quantify.

Species archetypes from the SAM showed different responses (occurrence probabilities) to the values of environmental variables. The responses among archetypes were reflective of the different characteristics of the individual species that comprised the archetypes and those species' habitat preferences (Hoffmayer et al. 2014). Species archetype 1 contained only one species (*R. venosa*) with a wide spatial range of substrate types (Figures 7, S.3, and S.5), and the responses of *R. venosa* to environmental variables (Table 4) were consistent with other studies reporting that *R. venosa* utilized multiple habitats related to rocks, sand, and silt soil within food-rich areas (Bondarev 2014). The optimal temperature (15–20°C) and depth (5–10 m) identified for *R. venosa* (i.e., SA1) from in situ observations (Bondarev 2013) were similar to our results.

Species archetype 2 showed lower occurrence probabilities than the other archetypes for most of the study area. Reef residence and the sedentary lifestyle of the sea urchin *Strongylocentrotus nudus* (Wu et al. 2016) and the rock-dependent *S. japonicus* (Han et al. 2016) may have caused the reef-oriented substrate preference displayed in Tables 3 and 4. Both are echinoderms with different feeding habits; sea urchins feed on algae and marine phanerogams, while sea cucumbers are detritivores and consume organic matter from the sediment (Parra-Luna et al. 2020). The goby *Stonogobiops pentafasciata* is a fish that feeds mostly on small-sized shrimp (Hung Liu et al. 2008). These three species have different feeding habits, so their inclusion in one archetype may be unduly influenced by the sampling

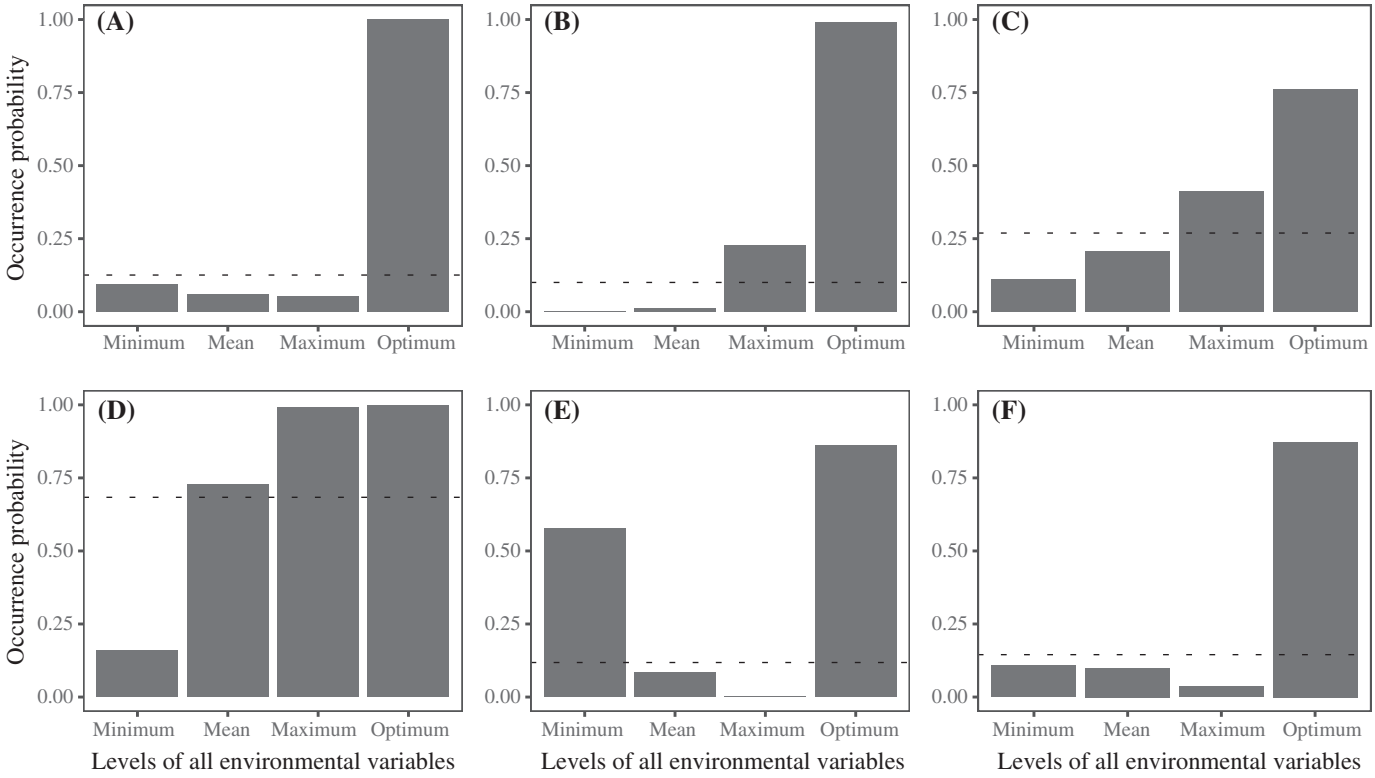

FIGURE 11. Occurrence probabilities of each species archetype (SA) when all environmental variables were fixed at their minimum, mean, maximum, and optimal values: **(A)** SA1, **(B)** SA2, **(C)** SA3, **(D)** SA4, **(E)** SA5, and **(F)** SA6. Optimal results are based on selecting the maximum values for the positive coefficients of parameters and the minimum values for the negative coefficients of parameters (Table S.4). Dashed lines represent the average of occurrence probabilities for the SAs identified by species archetype modeling.

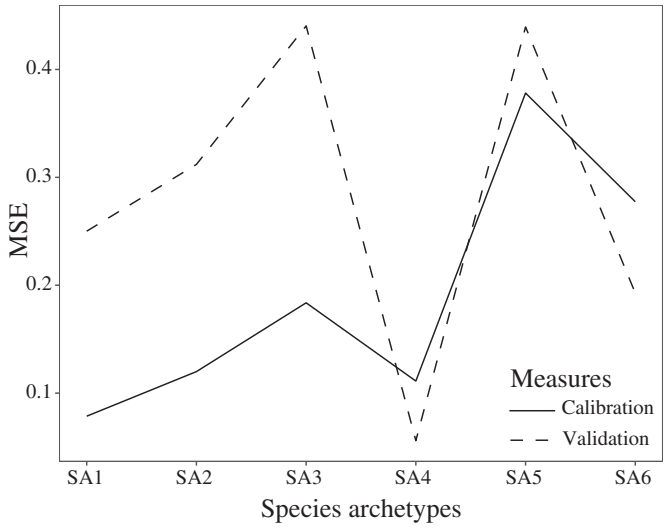

FIGURE 12. Values of mean square error (MSE) for species archetype model calibration (using the 13 surveys from June 2017 to May 2020) and validation (using data from the 14th survey [August 2020]).

method and differences in their distances to ARs and gravel habitats. Their generally low detection (from 12 to 19 sites; Table S.5) limits the robustness of the results.

Species archetypes 3, 4, and 6 showed strong relationships to environmental variables. Species in SA3 were well sampled by the visual census method because of the size and behavior of the Chameleon Goby (Boltachev et al. 2007) and because *A. amurensis* (Byrne et al. 1997) resides on the surface of reefs. Species archetypes 2 and 3 each had one fish species and either one or two echinoderms, and SA3 had a similar dependence of distance to different habitats as SA2. These taxa were assigned to different archetypes likely due to both having dependence on the visual data and because both species in SA3 preferred close proximity to ARs.

The four dominant species of SA4 have been broadly explored by researchers regarding their preference for complex habitat, especially ARs (Takeo 1999; Vazquez Archdale et al. 2003; Kim and Kang 2016; Zhang et al. 2018b). Korean Rockfish, Fat Greenling, and *C. japonica* had a preferred distribution at around 20–22°C (Yu et al. 2020), and Hannah et al. (2008) reported that the highest successful rate of *Sebastes* spp. capture occurred at depths less than 30 m, which was consistent with the responses of species in SA4 to environmental variables. The small values of RSE (i.e., good fit) and positive responses to bottom type score suggest that complex habitat is important for the

members of SA4. Two species (Korean Rockfish and Fat Greenling) exhibit significant overlap in their feeding and therefore likely may compete for resources, although their diets are distinct from those of *C. japonica* and *A. pectinifera* (Zhang et al. 2021). Without their common dependence on complex habitats, their assignment to the same archetype would have been less likely.

Species archetype 6 was comprised of fish species that are known to be associated with rocky habitats (Zhang et al. 2015; Yu et al. 2020), except for the Black Scraper *Thamnaconus modestus*, which tends to be located close to ARs but does not inhabit them (Takahashi et al. 2010). In our analysis, SA6 showed a positive relationship with the increasing complexity of substrate and with increasing proximity to ARs (Table 4); these habitat preferences were consistent with those reported in other studies (Takahashi et al. 2010; Zhang et al. 2015; Yu et al. 2020).

The responses of SA5 to environmental variables were opposite those of the other archetypes. For example, SA5 included burrowing species like the Japanese snapping shrimp *Alpheus japonicus*, whiparm octopus *Octopus variabilis*, and *O. oratoria* (Hamano and Matsuura 1984; Lü et al. 2013; Henmi et al. 2017); this is consistent with the observed preference of SA5 for soft, flat substrate and being located away from ARs. Goby fish (e.g., *A. hexanema*) and small shrimp (*Alpheus* and *Palaemon* spp.) from SA5 were reported to be the dominant species in winter or spring in the northeastern China Sea (Wang et al. 2012; Lu et al. 2019), which is consistent with the preference of SA5 for cool temperatures (Table 4). Species archetype 5 may be especially sensitive to the layout of AR deployments, such as appropriate spacing between AR monomers, to allow for sufficient physical space for their burrowing lifestyle. Consideration of habitat competition between rock-affiliated species and soft-sediment species is important to ensure effective AR layouts.

Influence of Sampling Methods

Trapping and visual census are common sampling methods used with ARs and can cause differences in the estimated species composition (Plumlee et al. 2020). Dominant species based on the two sampling methods in our analysis had high similarity that reflected common species in the northeastern China Sea—for example, *C. japonica* (Zhang et al. 2016) and the Korean Rockfish (Yu et al. 2020). However, the Chameleon Goby was classified into SA3 and occurred as a dominant species in the visual census but was rare in trap samples. The Chameleon Goby is a small-size species (Boltachev et al. 2007) that is undersampled by trapping (mesh size = 2 cm). Based on its diet of copepods and the larvae of shrimp and polychaetes (Kim and Yoon 2016), the presence of ARs likely provide food and shelter for the Chameleon Goby (Sun et al. 2013; Granneman and Steele 2014).

Combining data from multiple sampling methods, as was done in this analysis, leads to more robust results. Each method has certain strengths and limitations, and using multiple methods can result in complementary information. In our situation, the visual method provided effective sampling of boulder and AR substrate, while the trapping method enabled observations at gravel and mud habitats (SA1, SA2, SA5, and SA6 in Figure 8). Combining the information from trapping and visual sampling enabled a more complete depiction of how species and archetypes interact with ARs.

A general consideration is how the different catchabilities of the trapping and visual methods may influence the identification of the dominant species. Traps are a traditionally passive and fishery-dependent fishing gear that depends on the swimming capacity and behavior of epibenthic organisms but is limited because of its mesh size (Bohnsack et al. 1989). Visual census is an active, nondestructive fishing method that relies on diving and is influenced by turbidity, the patchiness of organisms, the photographic skills of the divers, and the ability to detect species in postprocessing of the videos (Harvey et al. 2004). These differences result in different sampling methods having strong effects on statistical methods (e.g., SAM) that are designed for grouping species. For example, *A. amurensis* from SA3 is a common benthic species residing in the surface of reefs with a low level of activity (Byrne et al. 1997; Michio et al. 2003) and, thus, is prone to be more readily detected by visual census. In contrast, the dominant species in SA4 are preferentially captured with trapping over visual census. Fat Greenling and Korean Rockfish of SA4 are large-sized, strong swimmers and are active. Due to the high abundance of *C. japonica* and *A. pectinifera* located in the boulder and AR areas, they are likely well sampled by both methods. To partially address sampling method differences, some analyses were done with the data treated separately, and when combined in an analysis, the data from both survey methods were transformed into presence/absence.

Comparison of Species Archetype Modeling, ISOPAM, and Other Classifications with Artificial Reefs

The consistency of archetypes from the SAM and the results of applying ISOPAM to the same data show that species co-occurrence is associated with similar responses to the environment. Viewing the consistency with SAM but starting with the ISOPAM groupings, species in ISOPAM group II were rock-associated fish, which all belonged to SA4; they showed a broad distribution pattern (Figure 9B versus Figure 6D). Species classified into ISOPAM groups I and III both belonged to SA5 of the SAM and were located some distance away from boulders and ARs (Figures 3; 7E; and 9A, C), which were the same responses of SA5 to substrate complexity. The ISOPAM

groups IVa and IVb combined (Table S.8) contained three species, all of which aggregated near the AR area.

There were also some differences between the SAM and ISOPAM approaches. For example, groups I and III from ISOPAM were separate, but according to the SAM they were combined into one archetype (SA5). Crustacean and cephalopod species from ISOPAM group I have similar distribution preferences and breeding habits, and they are reported to be the dominant species during winter or spring in the northeastern China Sea (Wang et al. 2012; Lu et al. 2019). However, the difference with *A. hexanema* from ISOPAM group III was that some species belonging to group I are prey of *A. hexanema* (Yamamoto 1942; Hamano and Matsuura 1984; Xue et al. 2013; Lu et al. 2019), which thus shows a different basis for classification based on co-occurrence by ISOPAM compared to the relationships with environmental variables used by the SAM. Furthermore, narrow or broad spatial distribution patterns could not be effectively utilized by ISOPAM, which were indicated by the species in SA1 (for narrow distribution), *A. pectinifera* and *C. japonica* in SA4 (for broad distribution), and the species in SA6 (for broad distribution) having low fidelity for grouping into one ISOPAM group. Grouping based on co-occurrence patterns versus relationships to environmental variables can provide both confirmatory information and insights into differences about spatial distributions and habitat usage.

Others have also proposed grouping schemes of species based on their habitat preferences in order to summarize the responses of the many fish that are influenced by ARs. Nakamura (1985) used fish taxonomy to delineate fish species associated with ARs into three types (A, B, and C): type A encompassed species that were located within the AR modules, type B included species that inhabited the local area around the modules, and type C comprised species that hovered above the reefs. Claudet et al. (2006) incorporated the influence of depth and habitat on fish assemblages in marine protected areas (MPAs) with rocky reefs and ARs using multivariate regression trees. The results of separated splits were different combinations of predicted fish abundances within or outside of the MPA, years before or after MPA establishment, and shallower or greater depths. Becker et al. (2019) classified pelagic and epibenthic fish around a multi-module AR area to investigate differences in fish assemblages between the bottom and pelagic zones. They separately reported two different archetypes in bottom and pelagic zones that each shared similar response to distance to the nearest AR.

All of these other classification schemes relied on the habitat preferences of the species and focused on fish. Our analysis included a wide diversity of taxa and species (i.e., beyond fish) and also relied on the shared responses of species to environmental conditions. We also tried to accommodate potential effects of interspecific interactions. For example, sympatric rockfishes (e.g., Korean Rockfish and Fat Greenling in SA4) that likely compete for food were identified into the same SA, but species involved in predator–prey interactions (Zhang et al. 2021), such as between crustaceans (e.g., *A. japonicus* or gladiator prawn *Palaemon ortmanni* in SA5) and rockfish (Korean Rockfish or Fat Greenling), were separated into different archetypes. Finally, we confirmed our results based on habitat usage (SAM results) by analyzing the same data but grouping based on co-occurrence patterns (ISOPAM results). Because it is difficult to compare across classification schemes because of site, data, and analysis differences, a comparative analysis that applies the suite of methods to the same data from multiple locations would be informative.

Future Modifications for Species Archetype Modeling

The SAM is based on GLMs, which assume that each environmental variable has a one-dimensional linear relationship with occurrence probabilities without any interactions or nonlinear effects. One possible influence is that the occurrence probability may be biased by the GLM when optimal conditions occur at intermediate values of environmental variables. For example, the optimal temperature of *R. venosa* was reported as 15–20°C (Bondarev 2013) for in situ observations, but our range extended from 6°C to 25°C, and the positive coefficient of SAM for the linear relationship indicated that *R. venosa* should prefer to distribute at 25°C. Potentially important information can be lost by reliance on linear relationships.

One area for modification to the SAM method would be to allow for using a model that can accommodate nonmonotonic and multi-dimensional responses of species to environmental variables. Because the SAM approach is currently restricted to mixture GLMs (Dunstan et al. 2013), Becker et al. (2019) only used SAMs for identifying archetypes for certain situations and then modeled the variance of abundance by generalized additive mixed models. Rooper et al. (2017) reported that species distribution models that use GAMs and machine-learning methods (e.g., boosted regression tree [BRT] models) can perform better in terms of prediction than GLMs. Hui et al. (2013) tested SAMs against separate GAMs and found that while GAMs predicted better than SAMs for abundant species, SAMs strongly outperformed GAMs for rarer species.

The SAM method is a statistical approach that is continuously being improved and further developed (Galanidi et al. 2016). In our present application, the SAM generally performed well but displayed high MSEs for SA3 and SA5 when validated. One possibility is overfitting, as most sites for SA3 depended on the visual census variable and

showed low sensitivity to many environmental variables (Figure 10). Species archetype 5 contained the largest number of species but also included a number of sites with low detections (Table S.5); this can also cause overfitting effects. We therefore conducted further analyses (not reported here) that involved fitting GAMs (Hastie and Tibshirani 1986) and the BRT model (Elith et al. 2006) and compared those results to the results from the SAM. When we compared the predicted occurrence probabilities of six archetypes with the same environmental variables, the BRT approach showed the best performance with the lowest MSEs among all archetypes. We suggest further analyses to update the core classification algorithm in the SAM to consider the sensitivity of responses to environmental variables inherent in different methods while simultaneously considering co-occurrence patterns or interactions of species with the species–environment information (Zhang et al. 2018a).

Archetypes and Fishery/Conservation Management

Archetypes and other methods that can accommodate the responses of many species can inform management about the full range of responses to expect when ARs are deployed. Reliance on the responses of focal or target species is useful for understanding how ARs can affect local ecological services (Xu et al. 2019) but is insufficient for understanding how other species will respond. When deploying ARs, finding suitable locations is a critical step (Golani and Diamant 1999). Methods that enable quantification of the benefits to the target species combined with methods that project the responses of other species are useful to ensure effective deployment.

Our analyses here demonstrated the feasibility of using the SAM method to predict occurrence probabilities of archetypes relative to different environmental conditions (including ARs). Our classification encompassed a wide range of common species in the AR area and simplified community composition, which could help to clarify the likely ecological responses to AR deployment. The various responses of the archetypes to environmental variables may help managers to guide AR location and arrangement and to have some expectations about how the ARs will perform as fishing sites or how conservation actions targeted at a species might affect other species. The importance of positive or negative responses of archetypes to ARs should be considered in designing AR deployments. Our general analysis approach can help to clarify the various purposes of AR deployment. For example, the analyses can be modified or expanded to accommodate consideration of how the number and layout of ARs would affect the suite of archetypes that indicate biodiversity, likely responses of target species (focus on specific archetypes), the degree of AR connectivity, and maintenance of key habitat types.

ACKNOWLEDGMENTS

This study was funded by the Project of National Key Research and Development Program of China (2019 YFD0901302). Sampling surveys were all conducted by members of the Fisheries Technology Laboratory at the Ocean University of China. We are grateful to Changdao Jiayi Precious Marine Product Co., Ltd. (a local marine ranching management company), for support. There is no conflict of interest declared in this article.

ORCID

Haolin Yu https://orcid.org/0000-0001-9716-6223

REFERENCES

Abelson, A. 2006. Artificial reefs vs coral transplantation as restoration tools for mitigating coral reef deterioration: benefits, concerns, and proposed guidelines. Bulletin of Marine Science 78:151–159.

Adie, H., I. Rushworth, and M. J. Lawes. 2013. Pervasive, long-lasting impact of historical logging on composition, diversity and above ground carbon stocks in Afrotemperate forest. Forest Ecology and Management 310:887–895.

Ardizzone, G. D., M. F. Gravina, and A. Belluscio. 1989. Temporal development of epibenthic communities on artificial reefs in the central Mediterranean Sea. Bulletin of Marine Science 44:592–608.

Barman, P., H. Yanan, and Q. Liu. 2020. Dynamic characteristics of community structure and seasonal variation of fishery species in the Bohai Sea, China. Applied Ecology and Environmental Research 18:817–837.

Becker, A., J. A. Smith, M. D. Taylor, J. McLeod, and M. B. Lowry. 2019. Distribution of pelagic and epi-benthic fish around a multi-module artificial reef-field: close module spacing supports a connected assemblage. Fisheries Research 209:75–85.

Becker, A., M. D. Taylor, and M. B. Lowry. 2017. Monitoring of reef associated and pelagic fish communities on Australia's first purpose built offshore artificial reef. ICES (International Council for the Exploration of the Sea) Journal of Marine Science 74:277–285.

Blanco, R. I., G. M. Naja, R. G. Rivero, and R. M. Price. 2013. Spatial and temporal changes in groundwater salinity in south Florida. Applied Geochemistry 38:48–58.

Bohnsack, J. A., D. L. Sutherland, D. E. Harper, D. B. McClellan, and C. M. Holt. 1989. The effects of fish trap mesh size on reef fish catch off southeastern Florida. Marine Fisheries Review 51:36–46.

Boltachev, A. R., E. D. Vasileva, and O. N. Danilyuk. 2007. First finding of Chinese Striped Trident Goby *Tridentiger trigonocephalus* (Perciformes, Gobiidae) in the Black Sea (estuary of the Tshemaya (Black) River, Sevastopol Harbor). Voprosy Ikhtiologii 47:847–850.

Bondarev, I. P. 2013. Ecomorphological analyses of marine mollusks' shell thickness of *Rapana venosa* (Valenciennes, 1846) (Gastropoda: Muricidae). International Journal of Marine Science 3:368–388.

Bondarev, I. P. 2014. Dynamics of *Rapana venosa* (Valenciennes, 1846) (Gastropoda: Muricidae) population in the Black Sea. International Journal of Marine Science 4:46–60.

Bortone, S. A., R. W. Hastings, and J. L. Oglesby. 1986. Quantification of reef fish assemblages: a comparison of several in situ methods. Gulf of Mexico Science 8:1–22.

Butman, C. A. 1987. Larval settlement of soft sediment invertebrates: the spatial scales of pattern explained by active habitat selection and the

emerging role of hydrodynamical processes. Oceanography and Marine Biology Annual Review 25:113–165.

Byrne, M., M. G. Morrice, and B. Wolf. 1997. Introduction of the northern Pacific asteroid *Asterias amurensis* to Tasmania: reproduction and current distribution. Marine Biology 127:673–685.

Chen, Q., H. R. Yuan, and P. M. Chen. 2019. Integrated response in taxonomic diversity and eco-exergy of macrobenthic faunal community to artificial reef construction in Daya Bay, China. Ecological Indicators 101:512–521.

Clark, S., and A. J. Edwards. 1999. An evaluation of artificial reef structures as tools for marine habitat rehabilitation in the Maldives. Aquatic Conservation: Marine and Freshwater Ecosystems 9:5–21.

Claudet, J., D. Pelletier, J. Y. Jouvenel, F. Bachet, and R. Galzin. 2006. Assessing the effects of marine protected area (MPA) on a reef fish assemblage in a northwestern Mediterranean marine reserve: identifying community-based indicators. Biological Conservation 130:349–369.

Coll, J., J. Moranta, O. Renones, A. Garcia-Rubies, and I. Moreno. 1998. Influence of substrate and deployment time on fish assemblages on an artificial reef at Formentera Island (Balearic Islands, western Mediterranean). Hydrobiologia 385:139–152.

Dunstan, P. K., S. D. Foster, and R. Darnell. 2011. Model based grouping of species across environmental gradients. Ecological Modelling 222:955–963.

Dunstan, P. K., S. D. Foster, F. K. C. Hui, and D. I. Warton. 2013. Finite mixture of regression modeling for high-dimensional count and biomass data in ecology. Journal of Agricultural, Biological, and Environmental Statistics 18:357–375.

Einbinder, S., A. Perelberg, O. Ben-Shaprut, M. H. Foucart, and N. Shashar. 2006. Effects of artificial reefs on fish grazing in their vicinity: evidence from algae presentation experiments. Marine Environmental Research 61:110–119.

Elith, J., C. H. Graham, R. P. Anderson, M. Dudik, S. Ferrier, A. Guisan, R. J. Hijmans, F. Huettmann, J. R. Leathwick, A. Lehmann, J. Li, L. G. Lohmann, B. A. Loiselle, G. Manion, C. Moritz, M. Nakamura, Y. Nakazawa, J. M. Overton, A. T. Peterson, S. J. Phillips, K. Richardson, R. Scachetti-Pereira, R. E. Schapire, J. Soberon, S. Williams, M. S. Wisz, and N. E. Zimmermann. 2006. Novel methods improve prediction of species' distributions from occurrence data. Ecography 29:129–151.

Foster, K. L., F. W. Steimle, W. C. Muir, R. K. Kropp, and B. E. Conlin. 1994. Mitigation potential of habitat replacement: concrete artificial reef in Delaware Bay—preliminary results. Bulletin of Marine Science 55:783–795.

Foster, S. D., P. K. Dunstan, F. Althaus, and A. Williams. 2015. The cumulative effect of trawl fishing on a multispecies fish assemblage in south-eastern Australia. Journal of Applied Ecology 52:129–139.

Galanidi, M., G. Kaboglu, and K. C. Bizsel. 2016. Predicting the composition of polychaete assemblages in the Aegean coast of Turkey. Frontiers in Marine Science 3:154.

Gallaway, B. J., L. R. Martin, R. L. Howard, G. S. Boland, and G. D. Dennis. 1981. Effects on artificial reef and demersal fish and macrocrustacean communities. Pages 237–299 *in* B. S. Middleditch, editor. Environmental effects of offshore oil production. Springer, Boston.

Godoy, E. A. S., T. C. M. Almeida, and I. R. Zalmon. 2002. Fish assemblages and environmental variables on an artificial reef north of Rio de Janeiro, Brazil. ICES (International Council for the Exploration of the Sea) Journal of Marine Science 59:S138–S143.

Golani, D., and A. Diamant. 1999. Fish colonization of an artificial reef in the Gulf of Elat, northern Red Sea. Environmental Biology of Fishes 54:275–282.

Granneman, J. E., and M. A. Steele. 2014. Fish growth, reproduction, and tissue production on artificial reefs relative to natural reefs. ICES (International Council for the Exploration of the Sea) Journal of Marine Science 71:2494–2504.

Guan, L., X. Shan, X. Jin, H. Gorfine, T. Yang, and Z. Li. 2020. Evaluating spatio-temporal dynamics of multiple fisheries-targeted populations simultaneously: a case study of the Bohai Sea ecosystem in China. Ecological Modelling 422:108987.

Guo, Z., L. Wang, W. Cong, Z. Jiang, and Z. Liang. 2021. Comparative analysis of the ecological succession of microbial communities on two artificial reef materials. Microorganisms 9:120.

Hamano, T., and S. Matsuura. 1984. Ecological studies on the Japanese mantis shrimp, *Oratosquilla oratoria* (DE HAAN). II. Egg laying and egg mass nursing behaviour in the Japanese mantis shrimp. Nsugaf 50:1969–1973.

Han, Q., J. K. Keesing, and D. Liu. 2016. A review of sea cucumber aquaculture, ranching, and stock enhancement in China. Reviews in Fisheries Science and Aquaculture 24:326–341.

Hannah, R. W., S. J. Parker, and K. M. Matteson. 2008. Escaping the surface: the effect of capture depth on submergence success of surface-released Pacific Rockfish. North American Journal of Fisheries Management 28:694–700.

Harvey, E., D. Fletcher, M. R. Shortis, and G. A. Kendrick. 2004. A comparison of underwater visual distance estimates made by scuba divers and a stereo-video system: implications for underwater visual census of reef fish abundance. Marine and Freshwater Research 55:573–580.

Hastie, T. J., and R. J. Tibshirani. 1986. Generalized additive models. Statistical Science 1:297–310.

Henmi, Y., C. Fujiwara, S. Kirihara, Y. Okada, and G. Itani. 2017. Burrow morphology of alpheid shrimps: case study of *Alpheus brevicristatus* and a review of the genus. Zoological Science 34:498–504.

Hixon, M. A., and J. P. Beets. 1989. Shelter characteristics and Caribbean fish assemblages: experiments with artificial reefs. Bulletin of Marine Science 44:666–680.

Hoffmayer, E. R., J. S. Franks, W. B. Driggers, J. A. McKinney, J. M. Hendon, and J. M. Quattro. 2014. Habitat, movements and environmental preferences of Dusky Sharks, *Carcharhinus obscurus*, in the northern Gulf of Mexico. Marine Biology 161:911–924.

Hui, F. K. C., D. I. Warton, S. D. Foster, and P. K. Dunstan. 2013. To mix or not to mix: comparing the predictive performance of mixture models vs. separate species distribution models. Ecology 94:1913–1919.

Hung Liu, H. T., D. Kneer, H. Asmus, and H. Ahnelt. 2008. The feeding habits of *Austrolethops wardi*, a gobiid fish inhabiting burrows of the thalassinidean shrimp *Neaxius acanthus*. Estuarine, Coastal and Shelf Science 79:764–767.

Kim, J. H., and J. C. Kang. 2016. The immune responses in juvenile rockfish, *Sebastes schlegelii* for the stress by the exposure to the dietary lead (II). Environmental Toxicology and Pharmacology 46:211–216.

Kim, J. Y., and J. M. Yoon. 2016. Food organisms of juveniles of *Tridentiger trigonocephalus* from the intertidal zone in the western coast of Korea. Journal of Fisheries and Marine Sciences Education 28:180–185.

Külköylüoğlu, O., M. Yavuzatmaca, D. Akdemir, and N. Sari. 2012. Distribution and local species diversity of freshwater Ostracoda in relation to habitat in the Kahramanmaraş Province of Turkey. International Review of Hydrobiology 97:247–261.

Lawesson, J. E. 2009. Effects of species partition on explanatory variables in direct gradient analysis—a case study from Senegal. Journal of Vegetation Science 8:409–414.

Leaper, R., P. K. Dunstan, S. D. Foster, N. S. Barrett, and G. J. Edgar. 2014. Do communities exist? Complex patterns of overlapping marine species distributions. Ecology 95:2016–2025.

Lima, J. S., I. R. Zalmon, and M. Love. 2019. Overview and trends of ecological and socioeconomic research on artificial reefs. Marine Environmental Research 145:81–96.

Lindquist, D. G., L. B. Cahoon, I. E. Clavijo, M. H. Posey, S. K. Bolden, L. A. Pike, S. W. Burk, and P. A. Cardullo. 1994. Reef fish stomach contents and prey abundance on reef and sand substrata associated with adjacent artificial and natural reefs in Onslow Bay, North Carolina. Bulletin of Marine Science 55:308–318.

Lu, K., W. Zhu, J. Liang, D. Li, Q. Dai, Z. Lu, and K. Xu. 2019. The relationship between shrimps community structure and environmental factors in Jiushan Islands waters. Journal of Zhejiang University (Sciences Edition) 46:65–77.

Lü, Z.-M., L.-Q. Liu, H. Li, C.-W. Wu, and J.-S. Zhang. 2013. Deep phylogeographic break among *Octopus variabilis* populations in China: evidence from mitochondrial and nuclear DNA analyses. Biochemical Systematics and Ecology 51:224–231.

McCullagh, P. 1989. Generalized linear models. European Journal of Operational Research 16:285–292.

Mellin, C., S. Andréfouët, and D. Ponton. 2007. Spatial predictability of juvenile fish species richness and abundance in a coral reef environment. Coral Reefs 26:895–907.

Michio, K., K. Kengo, K. Yasunori, M. Hitoshi, Y. Takayuki, Y. Hideaki, and S. Hiroshi. 2003. Effects of deposit feeder *Stichopus japonicus* on algal bloom and organic matter contents of bottom sediments of the enclosed sea. Marine Pollution Bulletin 47:118–125.

Miller, J. R., and R. J. Hobbs. 2007. Habitat restoration—do we know what we're doing? Restoration Ecology 15:382–390.

Miller, M. W. 2002. Using ecological processes to advance artificial reef goals. ICES (International Council for the Exploration of the Sea) Journal of Marine Science 59:S27–S31.

Murillo, F. J., E. Kenchington, G. Tompkins, L. Beazley, E. Baker, A. Knudby, and W. Walkusz. 2018. Sponge assemblages and predicted archetypes in the eastern Canadian Arctic. Marine Ecology Progress Series 597:115–135.

Nakamura, M. 1985. Evolution of artificial fishing reef concepts in Japan. Bulletin of Marine Science 37:271–278.

Parra-Luna, M., L. Martín-Pozo, F. Hidalgo, and A. Zafra-Gómez. 2020. Common sea urchin (*Paracentrotus lividus*) and sea cucumber of the genus *Holothuria* as bioindicators of pollution in the study of chemical contaminants in aquatic media. A revision. Ecological Indicators 113:106185.

Perkol-Finkel, S., and Y. Benayahu. 2005. Recruitment of benthic organisms onto a planned artificial reef: shifts in community structure one decade post-deployment. Marine Environmental Research 59:79–99.

Pinkas, L., M. Oliphant, and I. Iverson. 1971. Food habits of Albacore, Bluefin Tuna and Bonito in California waters. U.S. National Marine Fisheries Service Fishery Bulletin 152:1–105.

Plumlee, J. D., K. M. Dance, M. A. Dance, J. R. Rooker, T. C. Tin-Han, J. B. Shipley, and R. J. D. Wells. 2020. Fish assemblages associated with artificial reefs assessed using multiple gear types in the northwest Gulf of Mexico. Bulletin of Marine Science 96:655–678.

Pollock, L. J., R. Tingley, W. K. Morris, N. Golding, R. B. O'Hara, K. M. Parris, P. A. Vesk, and M. A. McCarthy. 2014. Understanding co-occurrence by modelling species simultaneously with a joint species distribution model (JSDM). Methods in Ecology and Evolution 5:397–406.

Reeds, K. A., J. A. Smith, I. M. Suthers, and E. L. Johnston. 2018. An ecological halo surrounding a large offshore artificial reef: sediments, infauna, and fish foraging. Marine Environmental Research 141:30–38.

Rooper, C. N., M. Zimmermann, and M. M. Prescott. 2017. Comparison of modeling methods to predict the spatial distribution of deep-sea coral and sponge in the Gulf of Alaska. Deep Sea Research Part I: Oceanographic Research Papers 126:148–161.

Sánchez-Jerez, P., B. M. Gillanders, S. Rodríguez-Ruiz, and A. A. Ramos-Esplá. 2002. Effect of an artificial reef in *Posidonia* meadows on fish assemblage and diet of *Diplodus annularis*. ICES (International Council for the Exploration of the Sea) Journal of Marine Science 59: S59–S68.

Sánchez-Jerez, P., and A. Ramos-Esplá. 2000. Changes in fish assemblages associated with the deployment of an antitrawling reef in seagrass meadows. Transactions of the American Fisheries Society 129:1150–1159.

Schmidtlein, S., L. Tichy, H. Feilhauer, and U. Faude. 2010. A brute-force approach to vegetation classification. Journal of Vegetation Science 21:1162–1171.

Schutter, M., M. Dorenbosch, F. M. F. Driessen, W. Lengkeek, O. G. Bos, and J. W. P. Coolen. 2019. Oil and gas platforms as artificial substrates for epibenthic North Sea fauna: effects of location and depth. Journal of Sea Research 153:101782.

Schwartz, G. 1978. Estimating the dimension of a model. Annals of Statistics 6:31–38.

Silva, K. J. P., and A. F. Souza. 2018. Common species distribution and environmental determinants in South American coastal plains. Ecosphere 9(6):e02224.

Smith, A. D. M., C. J. Brown, C. M. Bulman, E. A. Fulton, P. Johnson, I. C. Kaplan, H. Lozano-Montes, S. Mackinson, M. Marzloff, L. J. Shannon, Y. J. Shin, and J. Tam. 2011. Impacts of fishing low-trophic level species on marine ecosystems. Science 333:1147–1150.

Smith, J. A., W. K. Cornwell, M. B. Lowry, and I. M. Suthers. 2017. Modelling the distribution of fish around an artificial reef. Marine and Freshwater Research 68:1955–1964.

Sun, X., Z. Liang, J. Zou, and L. Wang. 2013. Seasonal variation in community structure and body length of dominant copepods around artificial reefs in Xiaoshi Island, China. Chinese Journal of Oceanology and Limnology 31:282–289.

Takahashi, H., A. Matsuda, T. Akamatsu, and N. Takagi. 2010. Spatial and temporal variation of the fish assemblage on a large artificial reef assessed using multiple-point stationary observations. Pages 135–140 *in* H. J. Ceccaldi, I. Dekeyser, M. Girault, and G. Stora, editors. Global change: mankind–marine environment interactions. Springer, Dordrecht, The Netherlands.

Takeo, K. 1999. Effects of sediment type and food abundance on the vertical distribution of the starfish *Asterina pectinifera*. Marine Ecology Progress Series 181:269–277.

Tichy, L., and M. Chytry. 2006. Statistical determination of diagnostic species for site groups of unequal size. Journal of Vegetation Science 17:809–818.

van Treeck, P., and H. Schuhmacher. 1999. Mass diving tourism—a new dimension calls for new management approaches. Marine Pollution Bulletin 37:499–504.

Ushiama, S., J. A. Smith, I. M. Suthers, M. Lowry, and E. L. Johnston. 2016. The effects of substratum material and surface orientation on the developing epibenthic community on a designed artificial reef. Biofouling 32:1049–1060.

Vazquez Archdale, M., K. Anraku, T. Yamamoto, and N. Higashitani. 2003. Behavior of the Japanese rock crab 'Ishigani' *Charybdis japonica* towards two collapsible baited pots: evaluation of capture effectiveness. Fisheries Science 69:785–791.

Wang, Y., J. Sun, E. Fang, B. Guo, Y. Dai, Y. Gao, H. Wang, X. Zhang, X. Xu, Y. Yu, and K. Liu. 2019. Impact of artificial reefs on sediment bacterial structure and function in Bohai Bay. Canadian Journal of Microbiology 65:191–200.

Wang, Y., C. Yu, Q. Chen, X. Chen, and J. Zheng. 2012. Community structure of fish in Zhoushan Fishing Ground and its adjacent waters in spring and summer. Yingyong Shengtai Xuebao 23:545–551. (In Chinese with English summary.)

Wang, Z.-H., J.-L. Mang, and S.-Y. Zhang. 2015. Comparison of pelagic and benthic fish assemblages in mussel farming habitat. Shengtaixue Zazhi 34:753–759. (In Chinese with English summary.)

Wu, Z. X., X. M. Zhang, H. M. Lozano-Montes, and N. R. Loneragan. 2016. Trophic flows, kelp culture and fisheries in the marine ecosystem of an artificial reef zone in the Yellow Sea. Estuarine, Coastal and Shelf Science 182:86–97.

Xu, M., L. Qi, L.-B. Zhang, T. Zhang, H.-S. Yang, and Y.-L. Zhang. 2019. Ecosystem attributes of trophic models before and after construction of artificial oyster reefs using Ecopath. Aquaculture Environment Interactions 11:111–127.

Xue, Y., Y.-P. Ji, and Q.-Y. Ma. 2013. Feeding ecology of *Amblychaeturichthys hexanema* in Jiaozhou Bay, China. Yingyong Shengtai Xuebao 24:1446–1452. (In Chinese with English summary.)

Yamamoto, T. 1942. On the ecology of *Octopus variabilis typicus* (Sasaki), with special reference to its breeding habits. Venus 12(1–3):9–20. (In Japanese with English summary.)

Yu, H., W. Yang, C. Liu, Y. Tang, X. Song, and G. Fang. 2020. Relationships between community structure and environmental factors in Xixiakou Artificial Reef Area. Journal of Ocean University of China 19:883–894.

Zhai, W.-D., H.-D. Zhao, J.-L. Su, P.-F. Liu, Y.-W. Li, and N. Zheng. 2019. Emergence of summertime hypoxia and concurrent carbonate mineral suppression in the central Bohai Sea, China. Journal of Geophysical Research: Biogeosciences 124:2768–2785.

Zhang, C., Y. Chen, B. Xu, Y. Xue, and Y. Ren. 2018a. Comparing the prediction of joint species distribution models with respect to characteristics of sampling data. Ecography 41:1876–1887.

Zhang, P., C. Li, W. Li, and X. Zhang. 2016. Effect of an escape vent in accordion-shaped traps on the catch and size of Asian paddle crabs *Charybdis japonica* in an artificial reef area. Chinese Journal of Oceanology and Limnology 34:1238–1246.

Zhang, R., H. Liu, Q. Zhang, H. Zhang, and J. Zhao. 2021. Trophic interactions of reef-associated predatory fishes (*Hexagrammos otakii* and *Sebastes schlegelii*) in natural and artificial reefs along the coast of north Yellow Sea, China. Science of the Total Environment 791:148250.

Zhang, X., H. Guo, S. Zhang, and J. Song. 2015. Sound production in Marbled Rockfish (*Sebastiscus marmoratus*) and implications for fisheries. Integrative Zoology 10:152–158.

Zhang, Y., Q. Xu, Q. Xu, J. Alós, H. Zhang, and H. Yang. 2018b. Dietary composition and trophic niche partitioning of Spotty-bellied Greenlings *Hexagrammos agrammus*, Fat Greenlings *H. otakii*, Korean Rockfish *Sebastes schlegelii*, and Japanese Seaperch *Lateolabrax japonicus* in the Yellow Sea revealed by stomach content analysis and stable isotope analysis. Marine and Coastal Fisheries: Dynamics, Management, and Ecosystem Science [online serial] 10:255–268.

Zuur, A. F., E. N. Ieno, and C. S. Elphick. 2010. A protocol for data exploration to avoid common statistical problems. Methods in Ecology and Evolution 1:3–14.

SUPPORTING INFORMATION

Additional supplemental material may be found online in the Supporting Information section at the end of the article.